Journal of Geochemical Exploration 206 (2019) 106356

Contents lists available at ScienceDirect

Journal of Geochemical Exploration

journal homepage: www.elsevier.com/locate/gexplo

Mass concentrations, seasonal variations, chemical compositions and element sources of PM_{10} at an urban site in Constantine, northeast Algeria

F. Bencharif-Madani, H. Ali-Khodja*, A. Kemmouche, A. Terrouche, K. Lokorai, L. Naidja, M. Bouziane

Laboratory of Pollution and Water Treatment, Department of Chemistry, Faculty of Exact Sciences, University of Mentouri Brothers-, Constantine 1 25017, Algeria

ARTICLE INFO

Keywords:
PM_{10}
Trace elements
Enrichment factor
Elemental ratio
Principal Component Analysis

ABSTRACT

This study presents for the first time, the results of a one-year measurement campaign on ambient PM_{10} (particulate matter with aerodynamic diameter < 10 μm) at an urban site at Zouaghi, in the south of Constantine, Algeria. The main objective of this work was to provide PM10 mass concentrations, a chemical characterization of atmospheric particles and their seasonal variation and to identify the sources of chemical elements in the PM_{10}. To accomplish the goal, enrichment factors (EFs), inter-element correlations, elemental ratios and principal component analysis (PCA) were used for the first time in Constantine. A total of 66 PM samples were collected during a sampling campaign which extended from January 2015 to February 2016. The PM_{10} samples were analyzed for a total of 48 elements by ICP-AES and ICP-MS for major elements and trace elements respectively. Enrichment factor analysis indicated that Pb, Sb, Cd, Bi, As, and Zn were mainly originated from anthropogenic sources. The ratios of Cu/Sb, Ca/Al, Zn/Pb, La/Ce and V/Ni were calculated and compared to those being reported in previous studies. A significantly higher Ca/Al ratio was dominant indicating the influence of construction dust, while a low Zn/Pb ratio was the consequence of high Pb concentrations resulting from the use of leaded gasoline. Principal component analysis allowed to identify four main groups of sources: crustal aerosol for Al, Fe, Ti, Li, Mg, Ba, Sr and rare earth elements (REEs) (47%), soil and road resuspension for Cr, As, S, P, V, Ca, Zn, Sn, Nb, K, Mg, Ba, Sr and Li (27%), traffic emission for Pb and Be (8%), and a metallurgical source for Cd and W (6%). The results of the source apportionment analysis indicate that natural dust originating from Saharan dust outbreaks (SDOs) and resuspended dust are the main sources of elements in PM_{10} in Constantine.

1. Introduction

The degradation of urban air quality caused by fine particulate matter has become a matter of great concern because of its harmful effects on human health. Epidemiological studies conducted in recent years have shown that, in urban areas, both the long-term and the short-term exposures to particulate matter with aerodynamic size below 10 μm (PM_{10}) are responsible for mortality and cardiopulmonary morbidity (Pope III and Dockery, 2006; Elichegaray et al., 2010; Kassomenos et al., 2013; Benaissa et al., 2016). For this reason, airborne PM concentrations are regulated by standards in view of these significant health impacts.

Desert regions of Northern Africa are the largest source of soil dust suspended in the atmosphere of the Earth. They account for 60–70% of global desert dust emissions (Rodrigez et al., 2011) and most of the mineral dust on a global scale is released to the atmosphere from arid or semiarid areas (Querol et al., 2009; Prospero et al., 2002), because of the acceleration of desertification processes in these regions, which is one of the consequences of climate change and human activities (Lal, 2001). Anthropogenic emissions do not exceed 10% of global particulate emissions, whereas natural primary emissions account for 84% of these (Querol et al., 2001).

It has been reported by several studies that some regions such as the Mediterranean sea and North Africa are strongly affected by intrusions of natural particles (desert dust), confirming that, each year, sand winds from the Sahara and Sahel carry large amounts of dust around the world (Querol et al., 2009; Rodrigez et al., 2011; Salvador et al., 2013; Salvador et al., 2014; Viana et al., 2014). Dust is transported across the Atlantic to the Americas and across North Africa and the Mediterranean Sea to Europe. These episodes of desert dust remain a recurring problem of air quality (Pérez et al., 2008), since they contribute to the exceedance of the daily limit values and annual averages of PM_{10} (Viana et al., 2014), thus affecting human health in the same way as $PM_{2.5}$ from other anthropogenic sources (WHO, 2016). In addition, Stafoggia

* Corresponding author.
E-mail address: halikhodja@umc.edu.dz (H. Ali-Khodja).

https://doi.org/10.1016/j.gexplo.2019.106356
Received 27 April 2019; Received in revised form 1 August 2019; Accepted 19 August 2019
Available online 28 August 2019
0375-6742/

et al. (2016) confirmed that desert dust outbreaks are an important risk factor to human health and that PM_{10} exposure caused by such natural events is not harmless.

The chemical composition of the particles is highly variable, consisting of inorganic compounds, organic matter (OM), elemental carbon (EC), marine aerosol and trace elements (Negral et al., 2008). Some components of particles are more harmful than others for human health. Among the inorganic compounds, there are metallic elements (Yadav and Satsangi, 2013) the most important of which are trace elements that are emitted by many sources such as geogenic materials, resuspension of soil dust, construction activities, traffic, oil combustion, incineration of waste and other industrial activities (Swaine, 2000).

The measurement of metallic elements concentrations in fine particles is of great interest for the evaluation of the exposure of the population, because many toxicological studies have shown that metals such as vanadium, iron, nickel, chromium, copper, zinc and manganese are among the components of fine particles which are potentially toxic (Pope III and Dockery, 2006).

It is important to note that, among other elements, mercury, lead, cadmium, chromium, nickel, cobalt are ubiquitous in the environment. They are considered carcinogenic, accumulate in the body and cause progressive toxicity (Pandey et al., 2017; Styszko et al., 2017). Moreover, several epidemiological studies have established links between human health and exposure to fine particles associated with metallic elements such as As, Au, Cd, Cr, Cu, Fe, Mn, Pb, Ni, Zn, etc. (Sanderson et al., 2014; Olawoyin et al., 2018). Although trace metals are very low in mass, they play a role in human health problems because they are commonly highly bioreactive (Moreno et al., 2006) and they accumulate in large quantities (Olawoyin et al., 2018).

It is often difficult to attribute the source of trace elements to a particular location and sometimes too much emphasis is placed on anthropogenic sources over natural sources, especially desert dust, which are not negligible. In this context, this study aims, for the first time and for a full year, to understand the variability of PM_{10} and forty eight trace elements that compose them at an urban site in the city of Constantine in Algeria. In this study, the seasonal variation of PM10 mass concentrations has been carefully studied. The anthropogenic and natural sources have been explored through enrichment factors (EFs). In addition, inter-element correlation, elemental ratios and principal component analysis (PCA) were performed to identify the sources of trace elements in PM_{10}.

2. Material and methods

2.1. Sampling site

This study was carried out at Zouaghi in the city of Constantine (36° 22′N, 6° 40′E) which is the third largest city in Algeria with about 0.6 million inhabitants. This city is located in northeastern Algeria at an altitude of 640 m above mean sea level. It is surrounded by twelve satellite towns located at distances from 6 to 34 km. The greater Constantine area has 1.3 million inhabitants. Most of this population is within a radius of 14 km. Air quality is impacted by several industrial and vehicular activities within and nearby the city. The main industrial activities include a cement plant and a mechanical pole a few kilometers north and south-east of the city respectively, ceramics, food, chemical industries, quarries, etc. The study area is illustrated in Fig. 1. The sampling site was located at Zouaghi which is an urban background site within the Faculty of Earth Sciences in the south of the city at a distance of 200 m from a very busy road, with a high flow of diesel buses, light-duty diesel trucks and gasoline passenger cars. The district of Zouaghi is a large urban residential area and can be considered as representative for the exposure of the general population. This site includes both building complexes and extensive estates of detached housing. The climate of Constantine is semi-arid Bourbia and Boucheriba, (2010) with great contrasts in temperature between summer and winter. It is cold in the winter with temperatures as low as −6C° and very hot in summer with peaks of up to 47 °C. The average rainfall varies from 500 mm to 700 mm per year.

2.2. Sample collection and chemical analysis

PM_{10} sampling was conducted over a period of one year between January 15, 2015 and February 03, 2016. A total of 66 samples were collected over the study period using a high volume sampler (Tisch Environmental, Model TE-6070), installed at a height of approximately 3 m from the ground. The sampling frequency was every sixth day for a 24 h period. PM_{10} samples were collected on 8 "× 10" quartz microfiber filters at a flow rate in the range 1.04–1.24 m^3/h.

Hourly meteorological data such as rainfall, temperature, pressure, humidity, wind direction and wind speed were extracted from the meteorological data archive of Ain-El-Bey weather station in Constantine which is located 1.5 km to the south of the sampling site.

The quartz fiber filters were carefully desiccated prior to and after the sampling to ascertain correct gravimetric estimation by an analytical balance (Shimadzu AUW 120D) with a sensitivity of 1 μg.

The samples were digested according to the protocol described by Kemmouche et al. (2017) in an acidic mixture of 1 ml HNO_3 and 2 ml HF in PFA flasks closed at 90 °C for at least 8 h. After cooling, 1 ml of $HClO_4$ was added. These PFA containers were then placed on a hot plate at 240 °C for complete evaporation. The dry residue obtained was then dissolved with 2.5 ml of HNO_3. The acidic solutions obtained were diluted in 25 ml of distilled water (Milli-Q). The solution obtained was filtered, stored and then analyzed by ICP-AES (IRIS Advantage TJA Solutions Thermo) and ICP-MS (X Series II Thermo) for major and trace elements, respectively. The blank filter was also extracted and analyzed in a similar manner to subtract the blank values from samples. All PM10 samples were analyzed for their elemental composition at IDAEA-CSIC laboratory in Barcelona. The XSERIES 2 ICPMS produces detection limits for virtually all analytes that are in the low ng/L (ppt) range. According to Moreno et al. (2010), the detection limits for some of the metal elements with both instruments are shown in Table 1.

A comparative study of different procedures conducted by Kemmouche et al. (2017) confirms that the use of a total extraction technique using HF which promotes the complete recovery of most elements is necessary for source apportionment studies, where a large number of elements are required, if the contribution of mineral dust is important. In this study, two bulk (requiring the use of HF) and three partial extraction procedures, one of which was assisted by microwave were applied using different acid mixtures. Five reference mineral-rich materials (Nist 1633b, UPM1648, NAT-7, SO-2 and SO-4) and 10 real PM10 filters collected from 15 January 2015 to 12 March 2015 in the present campaign were subjected to all five extraction protocols. Digested samples were acid-digested in duplicate. Both bulk extraction procedures were found to be very effective for elemental recoveries for most elements. Extraction protocols without HF lead to low extraction recoveries for most of the elements in all reference materials. Similar results were obtained with the urban 24-h PM10 samples. HF dissolution of filters was then preferred in order to ensure complete recovery in most cases. The dissolution procedure applied in this work was slightly more efficient than the other bulk extraction technique for most elements. The inherent good recoveries obtained with regard to reference materials allow validating at the same time IP-MS and ICP-AES measurements.

2.3. Source identification methods

To identify and apportion potential sources of PM_{10} over the study period, trajectory analysis, enrichment factors (EFs), inter-element correlations and principal component analysis (PCA) were used as they do not require a priori knowledge about the sources (Viana et al., 2008). Statistical treatment of data including Pearson correlation

Fig. 1. Study area and sampling site in Constantine (with wind rose diagram of the sampling period). (For interpretation of the references to colour in this figure legend, the reader is referred to the web version of this article.)

analysis and principal component analysis were carried out using the SPSS 20.0 statistical software.

2.3.1. Trajectory analysis and dust maps

The influence of atmospheric transport scenarios on the levels of PM was investigated by means of atmospheric backward trajectories using HYSPLIT model (Hybrid Single-Particle Lagrangian integrated trajectory) developed by NOAA air Resources Laboratory (Draxler and Hess, 1998). Daily 5-days back-trajectories were calculated at 12 h GMT at receptor points of 700, 1500 and 2500 m.a.s.l. They were used to determine the transport trajectory of air masses at the sampling site. This model has successfully been applied to interpret the influence of long-range transport on particle levels and other air pollutants (Garcia et al., 2018). The occurrence of African dust outbreaks was detected with the previous tool, coupled with the information from BSC-/DREAM dust maps (http://www.bsc.es/projects/earthscience/DREAM/). Maps on the daily dust load, the surface dust concentration and the vertical profile over the Sahara-Sahel region were collected as images from the BSC-DREAM8b (Dust REgional Atmospheric Model) model, operated by the Barcelona Supercomputing Center. The model predicts the atmospheric life cycle of the eroded desert dust (Aleksandropoulou and Lazaridis, 2012). The efficiency of this model to predict Saharan dust transport episodes was confirmed by Papanastasiou et al. (2010).

2.3.2. Enrichment factors (EFs)

Enrichment Factors (EF) were used to study the relative contribution of anthropogenic sources to those of natural origin. The calculation of element enrichment factors in our samples was based on the normalization of the element measured against a reference element. There is still no well-established rule for the choice of a reference element, except that it should not be affected by artificial factors (Hsu et al., 2016). Al, Si and Fe are the most commonly used elements for this

Table 1
Estimate of detection limits for PM components (Moreno et al., 2010).

Element	DL
$\mu g\,m^{-3}$	
Ca	0.004005
Fe	0.02017
K	0.02075
Na	0.10293
Mg	0.01697
$ng\,m^{-3}$	
P	0.00579
Ti	0.00218
V	0.00020
Mn	0.00079
Co	0.00004
Ni	0.00118
Cu	0.00278
Zn	0.03073
Ga	0.00004
Ge	0.00057
As	0.00007
Se	0.00008
Rb	0.00005
Sr	0.00043
Cd	0.00009
Sn	0.00201
Sb	0.00010
Ba	0.03708
La	0.00013
Ce	0.00032
Pb	0.00060
Bi	0.00004

purpose (Waheed et al., 2010; Huang et al., 2010); other less abundant elements have also been used in previous studies such as Mn, Sr, Zr and Ti (Cesari et al., 2012; Bouhila et al., 2015; Pasha and Alharbi, 2015).

The EF of a specific element (x) was calculated:

$$EF = \frac{\left(\frac{C_x}{C_{ref}}\right)sample}{\left(\frac{C_x}{C_{ref}}\right)crust}$$

where C_x is the concentration of the element of interest and C_{ref} is the concentration of a reference element. Al has been chosen as a reference element because of its abundance in the earth's crust and its stability (Al-Momani et al., 2005; Fang et al., 2006; Hsu et al., 2016) and also because it is commonly used in the literature for urban sites (Cesari et al., 2012; Padoan et al., 2016). The average composition of the upper continental crust (|UCC|) was obtained using the updated modified values provided by McLennan (2001). The UCC is used when no other database is available, although the best approach is to determine the EFs in relation to local soil composition (Budhavant et al., 2015).

Sodium is the reference element that is still used in the calculation of enrichment factors in relation to seawater (Al-Momani et al., 2005; Fang et al., 2006). Sodium is considered as a tracer element of marine spray that can be transported over long distances (Minguillón et al., 2012; Viana et al., 2014; Budhavant et al., 2015).

An E < 1 indicates that the element is depleted in the environment and therefore the natural sources are predominant. If the EF > 1, the element is relatively enriched in the environment, while, an EF > 5 indicates that a large part of the element can be attributed to anthropogenic sources (Gao et al., 2002; Enamorado-Baez et al., 2015; Budhavant et al., 2015). Elements can be considered highly enriched if EF > 100, moderately enriched when 10 < EF < 100 and less enriched in case EF < 10 (Mijic et al., 2010; Lim et al., 2010; Alleman et al., 2010; Yadav and Satsangi, 2013; Cheng et al., 2018).

2.3.3. Principal component analysis (PCA)

PCA is a multivariate method that has been commonly used in the last two decades to identify possible sources of particles (Karar and Gupta, 2007). It involves reducing the number of dimensions and removing the correlation between them (Elhadi et al., 2017), summarizing a multivariate data set into a few linear combinations of variables (called principal components). PCA results help to simplify the interpretation of positive and negative correlations between variables. This method was used to explore the relationship between variables using a rotation procedure called “Varimax” to maximize the explained variance. PCA is recognized as one of the most commonly used receptor techniques for source identification (Kalaiarasan et al., 2016). Previous studies have confirmed that trace elements in PM_{10} particles have various sources (Thurston and Splenger, 1985; Querol et al., 2006; Tian et al., 2010). Due to the relatively limited number of samples available versus the variables number (64 samples and 48 variables) and considering the condition $n > 30 + (V + 3)/2$, where n = number of samples and V = number of variables (Karar and Gupta, 2007), principal component analysis could be performed on PM_{10} data. After obtaining the data, PCA and Pearson correlation matrix were performed using SSPS statistical software, version 20.0. The measure of the Kaiser-Mayer-Olkin (KMO) index was followed by the execution of the PCA. We, then, proceeded to the next step only if the KMO value was 0.5 or above. In the present study, a value of 0.84 was obtained. PCA extracts variables into groups known as principal components (PCs). These components are arranged in descending order, from the largest to the smallest contributor, as precisely as possible with few major components (Elhadi et al., 2017). The post-rotation factor loadings are classified as strong (> 0.70), moderate (0.50–0.70) and weak < 0.50; weak loadings are suppressed (Wahid et al., 2013). PCA groups the variables as major components (PCs), with their eigenvalues, variability (%) and cumulative values (%) of individual and collective PCs to plot a graph from which the PCs with eigenvalue > 1 are retained (Elhadi et al., 2017).

3. Results and discussion

3.1. PM_{10} mass concentrations

The daily PM_{10} concentrations at the urban background site of study are shown in Fig. 2. The average mass concentration of PM_{10} was 55.7 $\mu g/m^3$. The maximum and the minimum concentrations were 135.9 and 5.0 $\mu g/m^3$ respectively. The annual mean concentration (55.7 $\mu g/m^3$) was almost 3 times higher than the WHO air quality guideline (20 $\mu g/m^3$), and more than the European Union's limit value for PM_{10} (40 $\mu g/m^3$). Nevertheless, this concentration was lower than the annual PM_{10} limit value of 80 $\mu g/m^3$ allowed in Algeria and was comparable to the concentrations recorded in previous studies carried out in several regions of the world such as Tunis, Sousse and Bizerte in

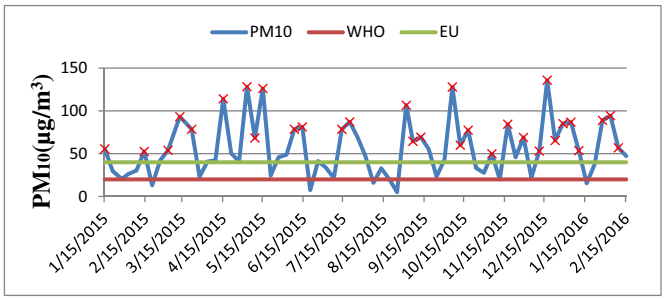

Fig. 2. Time variation of average daily PM_{10} concentrations. Red crosses indicate exceedance days with respect of the daily PM_{10} limit value (according to the Directive 2008/50/EC). (For interpretation of the references to colour in this figure legend, the reader is referred to the web version of this article.)

Table 2
PM_{10} concentration of the present study and studies elsewhere.

Study site	Year	PM_{10} (μg/m^3)	References
Zouaghi, Constantine, Algeria (urban)	Jan 2015–Feb 2016	55.7 ± 32	Present study
Daksi, Constantine, Algeria (urban)	March–May 2010	49	Terrouche et al. (2014)
Zouaghi, Constantine, Algeria (traffic)	March–Nov 2011	80.42	Terrouche et al. (2015)
Algiers, Algeria (urban)	Oct 2001–Sep 2002	61	Laïd et al. (2006)
Tunis(a), Sousse(b), Bizerte(c), Tunisia (urban)	2004–2010	(a) 90, (b) 58, (c) 80	Bouchlaghem and Nsom (2012)
Barcelone, Spain (urban)	March 1999–July 2000	49.5	Rodriguez et al. (2004)
Dar-essalem, Tanzania (urban)	May–June 2005	51	Mkoma et al. (2009)
Chengdu, China (urban)	Nov 2014–Oct 2015	173.6 ± 77.9	Cheng et al. (2018)
Riyadh, Saudi Arabia	Sep 2011–Sep2012	289.24 ± 228.5	Alharbi et al. (2015)
Aghia Paraskevi, Athens, Greece (urban)	June 2003–Dec 2008	34.1 ± 23.3	Pateraki et al. (2012)
Kolkata, India (residential/urban)	Nov 2003–Nov 2004	147.7 ± 97.3	Karar and Gupta (2006)
Piedmont region (Italy)	2001	59	Padoan et al. (2016)

Tunisia, Barcelona in Spain and Dar-essalem in Tanzania. They were; however, much lower than those recorded in Chengdu in China, Riyadh in Saudi Arabia, Athens in Greece and Kolkata in India (Table 2). The European daily limit value of 50 μg/m^3 (which should not be exceeded > 35 times a year), was exceeded 32 times out of the 64 sampling days, thus representing 50% of the samples (Fig. 2).

3.2. Seasonal variations and meteorological conditions

For the investigation of the seasonal variation, the year was divided into the four seasons: winter (December to February), spring (March to May), summer (June to August), autumn (September to November).

As shown in Table 3, the seasonal average PM_{10} concentrations were 44.57 μg/m^3 and 64.83 μg/m^3 in summer and spring respectively. Additionally, the average PM_{10} levels were 48.64 μg/m^3 and 59.83 μg/m^3 in winter and autumn respectively. There was no significant variation in PM_{10} concentrations between winter and summer on the one hand and between spring and fall on the other.

The sampling period from January 2015 to January 2016 was characterized by an almost total absence of precipitation during 2015 in January, February, April, June, July, September, October, November and December as shown in Fig. 3.

The highest seasonal PM_{10} levels observed during spring and fall were associated with low precipitation levels (Table 3). Such a condition prevents air renovation and promotes high resuspension due to soil dryness causing an increase in the concentrations of particles in the atmosphere. Exceedances of the PM_{10} limit values are due not only to anthropogenic emissions, but also to the long-range transport of desert dust. This seasonal cycle contrasts with several studies which reported high levels of PM_{10} in spring and summer compared to other seasons (Querol et al., 1998, 2009). The Sahara is one of the largest sources of dust on the planet, with North Africa being responsible for half of the global emissions of mineral dust (Pay et al., 2012).

The contribution of Saharan dust may lead to exceedances of the PM_{10} daily limit value of the European Union air quality standard (Matassoni et al., 2009), of the maximum number of days exceeding the EU daily limit (set at 35 exceedances per year) and of the annual average (set at 40 μg/m^3) (Bouchlaghem and Nsom, 2012). Two-thirds of exceedance days were affected by mineral dust which led either to widening the gap over the limit value or its exceedance at our sampling site (results not shown). Such events accounted for 33% of all the sampling days.

Table 3
Levels of precipitation and average PM_{10} concentrations for different seasons in Constantine.

Seasons	PM_{10} (μg/m^3)	Precipitations (mm)
Winter	48.64	84.48
Spring	64.83	22.90
Summer	44.57	104.04
Autumn	59.83	11.87

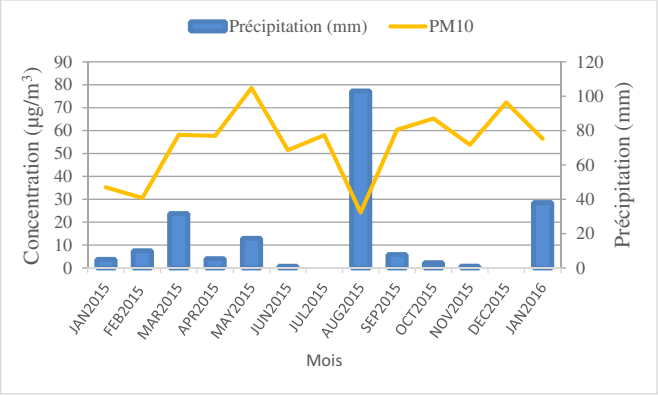

Fig. 3. Monthly variation of concentration of PM_{10} and precipitation levels.

The influence of atmospheric transport of air masses on the levels of particulate matter was investigated by means of back-trajectories analyses using the HYSPLIT Model (http://www.arl.noaa.gov), which was developed by the Atmospheric Resources Laboratory (NOAA). Backtrajectories were analyzed at altitudes of 750, 1500 and 2500 m on 15/04/2015, 03/05/2015, 15/05/2015, 01/09/2015 and 06/10/2015 which were days with the highest PM_{10} concentrations: 114, 128, 126, 107 and 128 μg/m^3, respectively. Saharn dust incursions were confirmed with BSC-/DREAM dust maps (http://www.bsc.es/projects/earthscience/DREAM/) (Fig. 4). The contribution of Saharan dust was in the range 80–160 μg/m^3.

The lowest PM_{10} concentration (5 μg/m^3) was observed during the month of august when an exceptional rainfall of 98 mm was recorded for just 1 day (25/08/2015). The consecutive leaching mechanism of the atmosphere significantly reduced the PM_{10} concentrations (Hieu and Lee, 2010). As shown in Fig. 5, both PM_{10} and trace metal element concentrations decreased sharply in the presence of rainfall. The considerable rainfall (98 mm) of August 25, 2015, led to a significant decrease of PM_{10} and trace elements concentrations which gradually increased afterwards.

3.3. Statistical analysis of elements concentrations

Arithmetic means, maximum and minimum values for the elements analyzed for the four seasons are presented in Table 4. Two groups can be distinguished: major elements (Al, Fe, Ca, K, Mg, Na, S) and trace elements (P, Li, Be, Sc, Ti, V, Cr, Mn, Co, Ni, Cu, Zn, Ga, Ge, As, Se, Rb, Sr, Yb, Zr, Nb, Cd, Sn, Sb, Cs, Ba, La, Ce, Pr, Nd, Sm, Gd, Dy, Hf, Ta, W, Tl, Pb, Bi, Th, U). Concentrations of major elements (Na, K, Ca, Mg, Fe, S and Al) were high in PM_{10}. Similar results were obtained in a previous study of Budhavant et al. (2015). The most abundant element was Ca

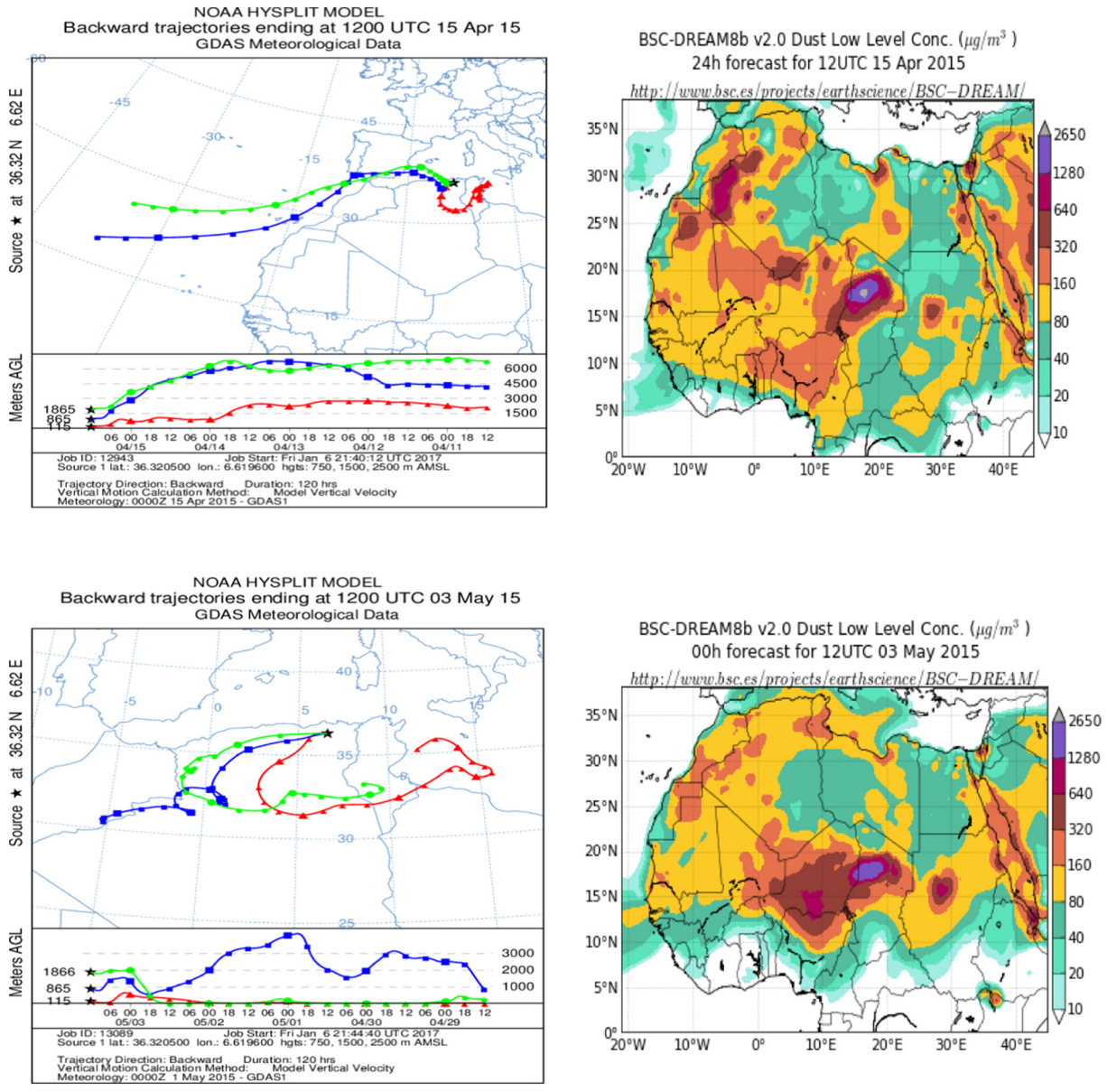

Fig. 4. Details of the intrusion of African dust on 15/04/2015, 03/05/2015, 15/05/2015 and 01/09/2015. (Left) Five days HYSPLIT back trajectoriesending at 12 UTC for 750, 1500 and 2500 m above sea level. (Right) image BSC-/DREAM dust maps (http://www.bsc.es/projects/earthscience/DREAM/).

(3290 ng/m^3) followed by Al (570 ng/m^3), S (400 ng/m^3), Fe (380 ng/m^3), Na (350 ng/m^3), Mg (200 ng/m^3) and K (190 ng/m^3). For trace elements, the average concentrations of Pb, Ti, Cu, P, Ba and Zn were 79.43, 33.08, 17.16, 16.86, 8.87 and 8.81 ng/m^3 respectively. They were higher than those of Mn, Zr, Sr, V and Cr which were < 6 ng/m^3.

The highest concentrations were reached in spring for 30 out of 48 elements (Table 5). Maximum concentrations for Ni, Cu, Ge and U were recorded in the summer. Maximum concentrations for Cd, Cs, Sm, Gd and Dy were observed in the fall season. Be, Pb, and Sb outmosted other elements in winter. Average seasonal concentrations of 29 elements were all under the unity and did not undergo, as such, significant seasonal variations. Only 12 metals had concentrations exceeding 1 ng/m^3. They were in descending order: Pb, Ti, Cu, P, Ba, Zn, Mn, Zr, Sr, V, Cr, and Ni.

Compared with other studies conducted around the world (Table 5), the annual mean concentration of PM_{10} in the present study was significantly lower than those recorded in Hankou (China), Agra (India) and Düzce (Turkey). It was more or less comparable to values observed in Barcelona (Spain), Cenica and To (Mexico). Most concentrations of metal elements were lower than those recorded in most studies, except for Pb which exceeded by far those recorded in Seville, Piedmont and Düzce (Amato et al., 2011; Padoan et al., 2016; Bozkurt et al., 2018) while remaining well below those reported for Hankou, Cenica and Agra (Querol et al., 2006; Querol et al., 2008; Singh and Sharma, 2012) in China, Mexico and India respectively. However, a study conducted in the town of Draria in Algiers reported lower concentrations of elements Cd, Sb, Sm, Ca, Cr, Mn and As than in the present study (Bouhila et al., 2015). Singh and Sharma (2012) reported higher concentrations of Ca, Fe, Mg, Na, S in a study conducted in the city of Agra in India. Ali-Khodja et al. (2008) reported higher concentrations of Cr, Mn, Co, Ni and Cu and Cd at an urban site in the nearby town of Didouche Mourad than the present study. This could be attributed to the size of dust collected as total suspended particulates in their study.

3.4. Enrichment factors

The enrichment factors of the 48 trace elements analyzed are shown in Fig. 6. In the present study, we can distinguish three main sources of

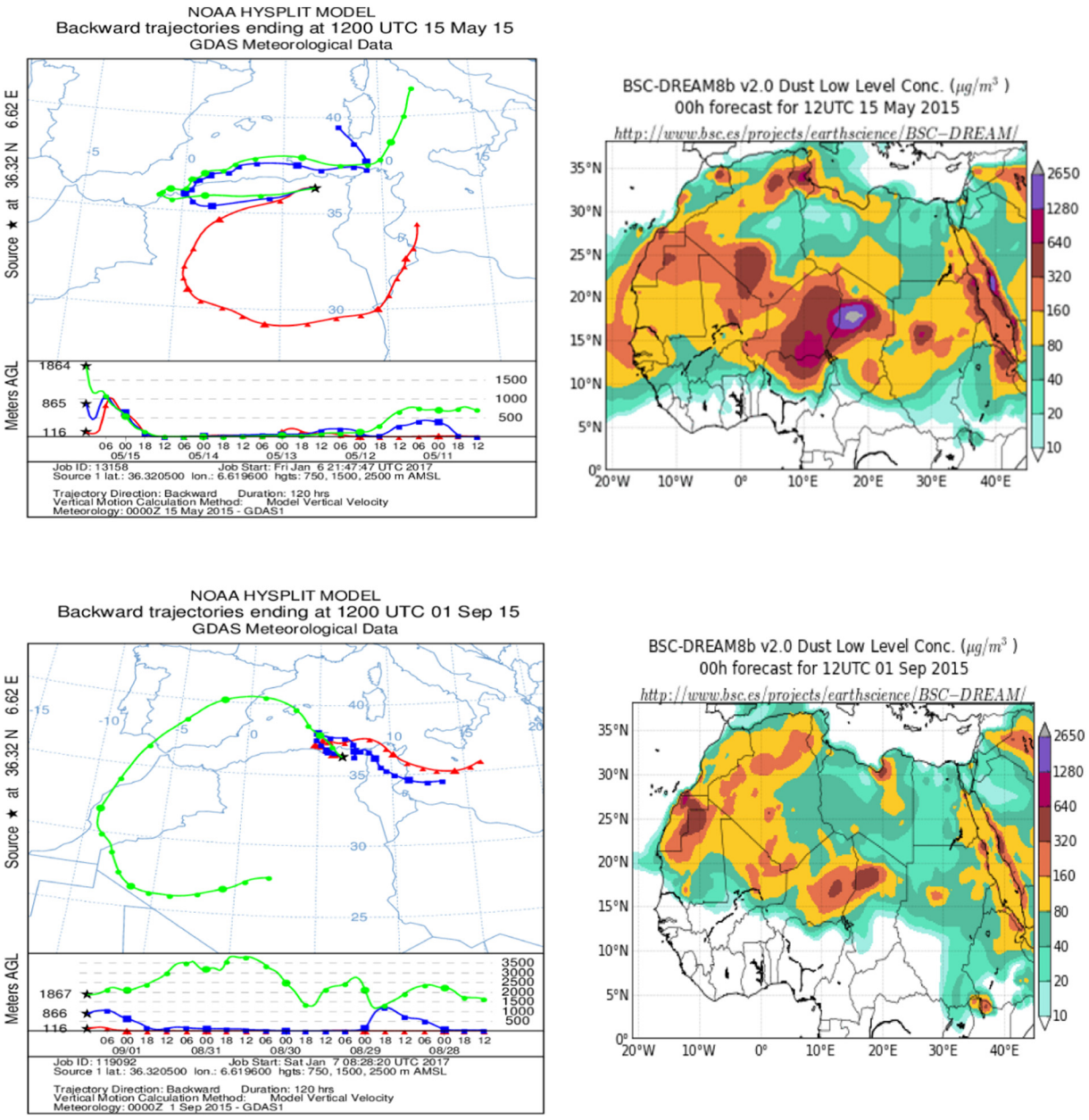

Fig. 4. (*continued*)

trace elements in PM_{10}, namely anthropogenic, mixed and crustal.

3.4.1. Elements associated with anthropogenic sources

Throughout the sampling period, Pb, Sb, Cd and Bi showed the highest EF, with values in the range 100–1000 (Fig. 6a). These elements are considered to present a strong anthropogenic component. For example, Pb is emitted by traffic in the sampling area as leaded gasoline is the major source of Pb in urban aerosol. Leaded gasoline is still used in Algeria (Terrouche et al., 2015; Naidja et al., 2018) despite its ban in most countries of the world (Singh and Sharma, 2012; Terrouche et al., 2015). Combustion of leaded gasoline continues to be the major source of atmospheric Pb emissions worldwide (Pacyna and Pacyna, 2001). Antimony (Sb) has also a high enrichment factor (EF $>$ 100). The use of antimony alloys in various components of automobiles and vehicles results in a significant increase in Sb emissions in the environment (Belzile et al., 2011). Moreover, antimony is a low boiling point element, which can therefore be emitted in the form of particles or submicron gases during combustion processes. This element is commonly associated with high temperature anthropogenic processes, such as metal smelting, combustion and waste incineration which are considered as the main sources of antimony emission into the atmosphere (Filella et al., 2009). Antimony is a potential tracer for waste incineration (Christian et al., 2010). It is worthwhile to note that the waste incinerator of the region was located 13 km north of the monitoring site. In the past, brake pads were made from asbestos. With the removal of asbestos, pads are now made from other materials, such as Ba and Sb sulfates, Mg and Cr oxides and other metal powders (Dongarrà et al., 2009). For Cu, As, Zn, Sn, Ca, the values of EFs are in the range of 10–100 (Fig. 6a), indicating that these elements are mainly anthropogenic for all seasons. The high EFs of Zn, Sb, Bi, Cd and Cu may be due to the influence of traffic in the sampling area. These elements are generally associated with emissions other than exhaust gases, particularly tire abrasion, brake wear and pavement degradation (Amato et al., 2011; Minguillón et al., 2012). Another major source of Zn and Cd is the incineration of household waste. Some fossil fuels may contain arsenic which can be emitted during combustion (Enamorado-

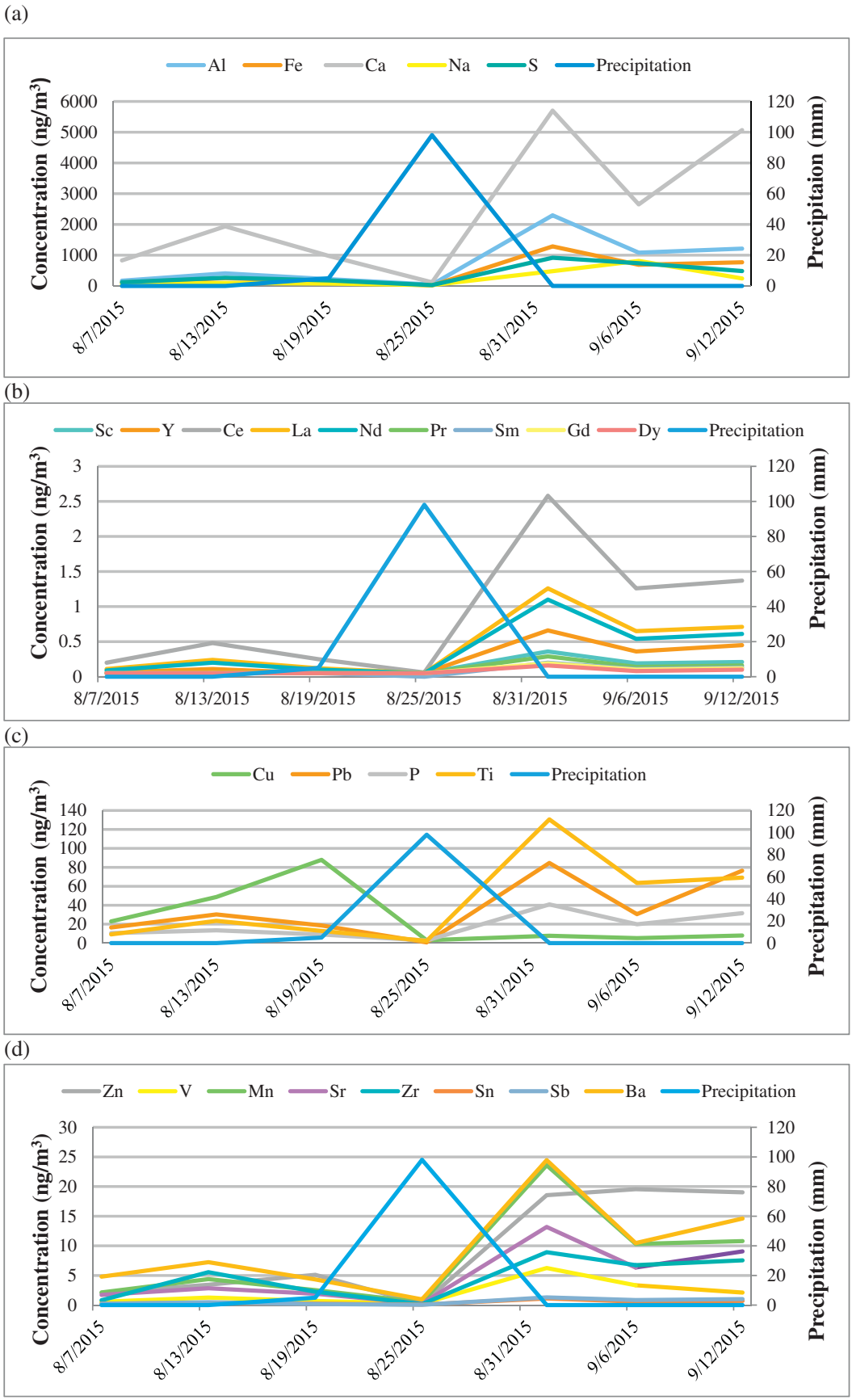

Fig. 5. Concentration of (a) five major elements (Al, Fe, Ca, Na, S), (b) REEs, (c) and (d) twelve trace elements (Cu, Pb, P, Ti, Zn, V, Mn, Sr, Zr, Sn, Sb, Ba) during a heavy rainfall event (98 mm only for the day of 25/08/2015).

Table 4
Average, standard deviation, minimum and maximum concentrations of PM_{10} and the different species for different seasons.

	Annual		Winter	Spring	Summer	Autumn
	Mean ± SD	Range	Mean ± SD	Mean ± SD	Mean ± SD	Mean ± SD
µg/m^3						
PM_{10}	55.7 ± 32.03	4.99–135.89	48.64 ± 16.78	64.83 ± 9.75	44.57 ± 14.61	59.83 ± 4.69
Al	0.57 ± 0.62	0.03–2.55	0.45 ± 0.09	0.76 ± 0.15	0.54 ± 0.16	0.55 ± 0.30
Ca	3.29 ± 3.15	0.01–11.95	3.27 ± 2.17	5.76 ± 0.61	3.30 ± 1.44	1.32 ± 0.70
Fe	0.38 ± 0.36	0.02–1.41	0.35 ± 0.10	0.52 ± 0.07	0.34 ± 0.10	0.35 ± 0.13
K	0.19 ± 0.16	0.01–0.75	0.14 ± 0.06	0.27 ± 0.06	0.17 ± 0.05	0.22 ± 0.09
Mg	0.2 ± 0.19	0.01–0.78	0.18 ± 0.12	0.35 ± 0.06	0.18 ± 0.06	0.14 ± 0.09
Na	0.35 ± 0.43	0.01–2.66	0.42 ± 0.41	0.61 ± 0.14	0.23 ± 0.09	0.24 ± 0.19
S	0.4 ± 0.33	0.01–1.15	0.38 ± 0.26	0.59 ± 12.43	0.49 ± 0.21	0.22 ± 0.16
ng/m^3						
P	16.86 ± 21.76	0.1–144.1	10.86 ± 6.59	34.34 ± 12.43	19.09 ± 5.38	5.49 ± 7.03
Li	0.35 ± 0.34	0.05–1.32	0.29 ± 0.10	0.51 ± 0.07	0.34 ± 0.10	0.29 ± 0.15
Be	0.07 ± 0.02	0.05–0.10	0.10 ± 0.00	0.06 ± 0.01	0.05 ± 0.00	0.07 ± 0.02
Sc	0.11 ± 0.09	0.04–0.51	0.11 ± 0.01	0.13 ± 0.02	0.08 ± 0.02	0.13 ± 0.05
Ti	33.08 ± 35.60	2–153.61	24.41 ± 5.04	45.23 ± 8.96	31.86 ± 9.46	32.28 ± 16.77
V	1.86 ± 1.63	0.05–6.45	1.49 ± 1.12	2.83 ± 0.63	2.11 ± 0.81	1.33 ± 0.77
Cr	1.85 ± 1.70	0.05–8.45	2.26 ± 1.68	2.59 ± 0.90	2.00 ± 0.47	0.94 ± 0.45
Mn	5.99 ± 5.76	0.05–23.59	4.29 ± 1.12	8.57 ± 1.54	6.17 ± 1.65	5.39 ± 2.19
Co	0.14 ± 0.13	0.05–0.55	0.13 ± 0.02	0.18 ± 0.03	0.13 ± 0.03	0.14 ± 0.06
Ni	1.24 ± 1.18	0.09–4.03	0.32 ± 0.07	1.62 ± 0.45	2.65 ± 0.32	0.53 ± 0.43
Cu	17.16 ± 21.75	0.15–93.41	7.64 ± 4.47	20.25 ± 6.35	41.90 ± 10.44	2.46 ± 1.34
Zn	8.81 ± 6.78	0.15–34.25	11.27 ± 3.80	11.48 ± 3.79	5.77 ± 1.83	7.40 ± 3.57
Ga	0.15 ± 0.14	0.05–0.59	0.14 ± 0.02	0.19 ± 0.04	0.14 ± 0.04	0.14 ± 0.07
Ge	0.12 ± 0.07	0.05–0.3	0.08 ± 0.02	0.12 ± 0.02	0.18 ± 0.03	0.10 ± 0.03
As	0.46 ± 0.36	0.05–1.45	0.56 ± 0.30	0.64 ± 0.09	0.45 ± 0.14	0.28 ± 0.11
Se	0.2 ± 0.17	0.05–0.97	0.22 ± 0.15	0.25 ± 0.02	0.18 ± 0.03	0.18 ± 0.09
Rb	0.72 ± 0.73	0.05–2.89	0.49 ± 0.14	0.95 ± 0.17	0.72 ± 0.23	0.80 ± 0.15
Sr	4.98 ± 5.05	0.1–22.36	3.75 ± 1.51	8.79 ± 1.27	4.92 ± 1.74	2.93 ± 1.83
Yb	0.18 ± 0.18	0.05–0.77	0.13 ± 0.03	0.24 ± 0.06	0.16 ± 0.04	0.18 ± 0.09
Zr	5.2 ± 3.10	0.16–11.05	5.09 ± 3.19	6.72 ± 0.40	4.81 ± 1.29	4.81 ± 2.19
Nb	0.2 ± 0.18	0.05–0.78	0.26 ± 0.13	0.27 ± 0.07	0.15 ± 0.04	0.15 ± 0.07
Cd	0.22 ± 0.19	0.05–1.08	0.21 ± 0.06	0.18 ± 0.05	0.08 ± 0.02	0.41 ± 0.09
Sn	0.68 ± 0.58	0.05–2.44	0.89 ± 0.33	0.89 ± 0.14	0.54 ± 0.19	0.47 ± 0.27
Sb	0.85 ± 0.67	0.05–2.76	1.18 ± 0.41	0.90 ± 0.03	0.65 ± 0.29	0.66 ± 0.14
Cs	0.19 ± 0.31	0.04–1.84	0.17 ± 0.15	0.09 ± 0.01	0.12 ± 0.05	0.39 ± 0.38
Ba	8.87 ± 6.97	0.3–26.13	8.43 ± 3.28	11.88 ± 1.24	9.42 ± 3.24	6.45 ± 1.58
La	0.32 ± 0.35	0.05–1.59	0.23 ± 0.07	0.42 ± 0.09	0.31 ± 0.08	0.33 ± 0.17
Ce	0.65 ± 0.74	0.05–3.28	0.45 ± 0.13	0.83 ± 0.18	0.60 ± 0.16	0.73 ± 0.41
Pr	0.1 ± 0.07	0.05–0.37	0.12 ± 0.03	0.11 ± 0.02	0.08 ± 0.01	0.11 ± 0.01
Nd	0.28 ± 0.31	0.05–1.4	0.22 ± 0.05	0.37 ± 0.07	0.26 ± 0.07	0.29 ± 0.15
Sm	0.09 ± 0.31	0.1–0.27	0.08 ± 0.03	0.08 ± 0.01	0.06 ± 0.01	0.14 ± 0.03
Gd	0.08 ± 0.04	0.05–0.24	0.07 ± 0.03	0.08 ± 0.01	0.06 ± 0.01	0.12 ± 0.01
Dy	0.08 ± 0.03	0.05–0.17	0.07 ± 0.02	0.07 ± 0.01	0.06 ± 0.01	0.11 ± 0.01
Hf	0.21 ± 0.10	0.05–0.38	0.20 ± 0.10	0.26 ± 0.03	0.20 ± 0.04	0.22 ± 0.07
Ta	0.09 ± 0.03	0.05–0.19	0.10 ± 0.00	0.08 ± 0.01	0.06 ± 0.00	0.10 ± 0.00
W	0.08 ± 0.02	0.05–0.12	0.09 ± 0.02	0.07 ± 0.01	0.06 ± 0.01	0.09 ± 0.01
Tl	0.08 ± 0.08	0.05–0.64	0.08 ± 0.02	0.06 ± 0.01	0.07 ± 0.01	0.09 ± 0.05
Pb	79.43 ± 69.75	0.8–260.24	138.41 ± 22.98	69.67 ± 7.66	35.81 ± 12.67	67.90 ± 29.74
Bi	0.1 ± 0.00	0.07–0.1	0.10 ± 0.00	0.10 ± 0.00	0.10 ± 0.00	0.10 ± 0.00
Th	0.11 ± 0.09	0.02–0.42	0.10 ± 0.03	0.12 ± 0.03	0.11 ± 0.02	0.13 ± 0.03
U	0.09 ± 0.04	0.05–0.21	0.06 ± 0.02	0.08 ± 0.03	0.12 ± 0.01	0.08 ± 0.02

Baez et al., 2015). High values for Pb and Zn have already been reported by Megido et al. (2016) who related Cu, Sn, Sb and Bi to brake wear. Brake abrasion is thought to be one of the most important sources of Sb and Cu in PM (Iijima et al., 2009; Amato et al., 2011; Lage et al., 2016). Calcium may have different sources as it may originate from sea spray (Megido et al., 2016), construction and demolition works (Amato et al., 2009a), road dust resuspension (Amato et al., 2011), cement industries (Morishita et al., 2011; Alharbi et al., 2015), vehicular emissions and iron and steel plants (Mooibroek et al., 2016). Mineral industries such as the cement and ceramic brick plants as well as a stone quarry which are strong emitters of calcium (Yatkin and Bayram, 2008) are situated 13 km north north of the sampling site which is in the wake of prevailing north westerly winds. Calcium is highly enriched with respect to seawater (EF > 100) (Fig. 6c) but is moderately enriched with respect to the earth's crust (EF > 10). This reflects not only the contribution of soil dust resuspension (Amato et al., 2011), but also the impact of other complementary human activities such as the use of cement in nearby construction works (Wang et al., 2008; Dall'Osto et al., 2012).

3.4.2. *Elements associated with mixed sources*

Relatively lower EFs values (ranging from 1 to 10) were obtained for Ti, Fe, Si, Mn, P, Na, Mg, Co, Sr, Ba, Ni, V, Cr and Cs for all seasons. In this study silicon was not measured and was indirectly determined using the measured aluminum concentration multiplied by a factor of 4.6 (Miller-Schulze et al., 2015). These elements come from mixed sources and mainly from crustal and marine ones as the contribution of the anthropogenic counterpart is smaller (Dai et al., 2015). Iron, Ti, Si and P are related to crustal sources (Dall'Osto et al., 2012; Dai et al., 2015) and Na, Mg and Sr to marine sources (Fig. 6c) (Dall'Osto et al., 2012). The resuspension of particles is the dominant source of elements Ba, Mn, Cs (Cheng et al., 2018; Amato et al., 2009a) and Cr (Dai et al.,

Table 5
Mean PM_{10} (μg/m^3), major (μg/m^3) and trace elements levels (ng/m^3) from different cities in the world compared with the data obtained in this study, *for elements in ng/m^3.

	Present study[a]	Hankou, China[b]	Barcelona, Spain[c]	Piedmont, Italy[d]	Mexico[e]		Algiers, Algeria[f]	Agra, India[g]	Düzce, Turkey[h]	Constantine Algeria[i]
					Cenica	To				
PM_{10}	55.7	156	42	65	52	52	–	155.25	86.4	
Al	0.57	3.7	0.42	0.38	1.58	2	–	–	5.3	
Ca	3.29	5.0	1.4	1.04	1	2	0.27	7.23	2.5	
Fe	0.38	3	0.6	2.48	1	1	0.54	3.96	–	
K	0.19	4	0.3	0.39	1	1	0.37	4.36	–	
Mg	0.2	1	0.3	0.52	0.5	0.4	–	1.71	–	
Na	0.35	1	1	–	0.5	0.5	–	3.97	–	
S	0.4	–	1	–	1.66	5	–	4.65	–	
P*	16.86	137	0.02	–	–	–	–	–	–	
Li*	0.35	4	0.5	–	–	–	–	–	–	
Be*	0.07	–	–	–	–	–	–	–	–	
Sc*	0.11	1	0.9	–	–	–	0.15	60	1.1	
Ti*	33.08	214	29	26.7	114	81	–	–	–	
V*	1.86	7	9	2.77	19	25	4.36	42.35	2.6	
Cr*	1.85	11	5	12.1	1	4	1.43	70	14.7	16
Mn*	5.99	116	15	28.4	20	32	4.25	–	29.0	50
Co*	0.14	1	0.2	0.65	0.5	1	0.71	–	0.7	14
Ni*	1.24	4	4.6	5.97	3	5	–	50	11.8	11
Cu*	17.16	40	28	67.3	75	110	–	130	12.4	24
Zn*	8.81	676	81	83	100	482	10.0	630	115.3	
Ga*	0.15	5	0.2	–	–	–	–	–	–	
Ge*	0.12	1	–	–	–	–	–	–	–	
As*	0.46	66	0.7	1.03	5	6	0.19	50	1.8	
Se*	0.2	11	0.9	–	–	–	0.15	–	0.9	
Rb*	0.72	18	0.9	–	–	–	–	110	–	
Sr*	4.98	37	4	239	9	16	12.0	–	–	
Yb*	0.18	1	–	–	–	–	–	–	–	
Zr*	5.2	15	12	3.21	–	–	–	–	–	
Nb*	0.2	1	–	–	–	–	–	–	–	
Cd*	0.22	4	0.2	1.1	1	3	0.03	23.50	0.6	1
Sn*	0.68	10	6	–	–	–	–	–	6.0	
Sb*	0.85	16	2.9	10.1	–	–	0.71	–	6.3	
Cs*	0.19	14	–	–	–	–	–	–	–	
Ba*	8.87	2	–	40.2	–	–	–	90	21.4	
La*	0.32	58	0.3	2.39	–	–	0.66	–	–	
Ce*	0.65	2	0.7	2.57	–	–	1.30	–	–	
Pr*	0.1	4	–	–	–	–	–	–	–	
Nd*	0.28	0.4	–	–	–	–	–	–	–	
Sm*	0.09	2.0	–	–	–	–	0.07	–	–	
Gd*	0.08	0.2	–	–	–	–	0.22	–	–	
Dy*	0.08	0.1	–	–	–	–	–	–	–	
Hf*	0.21	0.01	–	–	–	–	0.04	–	–	
Ta*	0.09	1	–	–	–	–	–	–	–	
W*	0.08	0.1	–	–	–	–	–	–	–	
Tl*	0.08	2	–	–	–	–	–	–	–	
Pb*	79.43	409	13	13.7	3	111		260	21.1	46
Bi*	0.1	11	0.4	–	–	–		–	0.3	
Th*	0.11	1	–	–	–	–	–	–	–	
U*	0.09	0.3	0.13	–	–	–	–	–	–	

[a] Constantine (urban receptor site); The present study.
[b] Hankou (urban); Querol et al. (2006).
[c] Barcelone (urban background); Amato et al. (2011).
[d] Piedmont (urban); Padoan et al. (2016).
[e] Cenica and To (urban background); Querol et al. (2008).
[f] Algiers (suburban); Bouhila et al. (2015).
[g] Agra (urban); Singh and Sharma (2012).
[h] Düzce (urban); Bozkurt et al. (2018).
[i] Constantine (urban); Ali-Khodja et al. (2008).

2015). These elements are sometimes associated with road dust (Kara et al., 2014) as it combines brake wear emissions and abrasion of mechanical parts of vehicles, and thus contaminates soil dust with anthropogenic metals (Sternbeck et al., 2002). The presence of Ni and V in urban air is generally associated with fuel-oil combustion (Moreno et al., 2010a; Pandolfi et al., 2011; Dall'Osto et al., 2012). However, Fe has a relatively high concentration but a lower enrichment factor (< 5), suggesting that it is originated mainly from natural processes, such as wind-driven soil dust resuspension (Feng et al., 2009; Amato et al., 2011). Iron is also associated with human activities such as industrial processes, abrasion of metallic materials and traffic-related sources (Genga, 2012).

3.4.3. *Elements associated with crustal sources*

In addition to Ti, Si and Fe, the lanthanides also have EFs close to 1. In terms of abundance, the most common lanthanides are ranked: Ce > La > Pr > Sm > Yb > Lu (Hsu et al., 2016). The data collected at our site also reflect the same order and confirm that

(a)

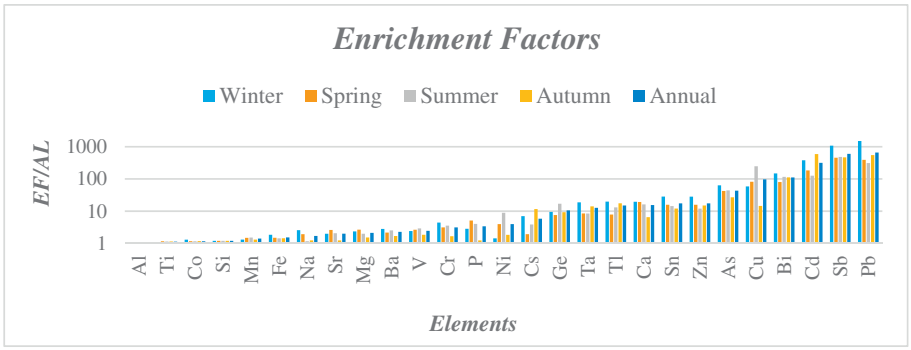

(b)

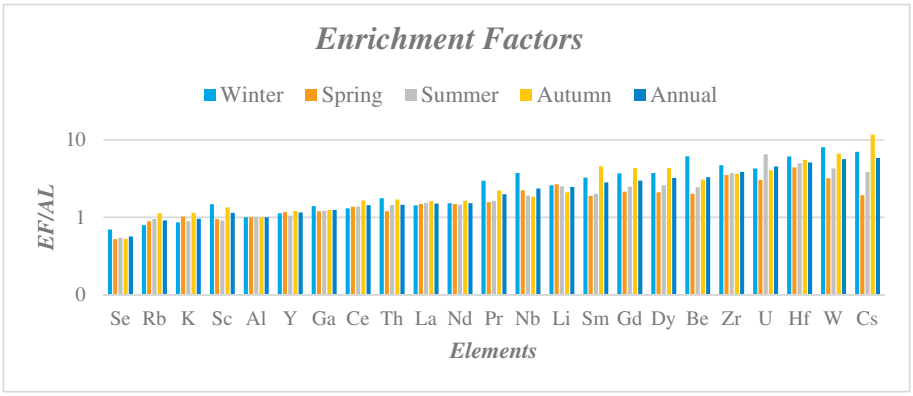

(c)

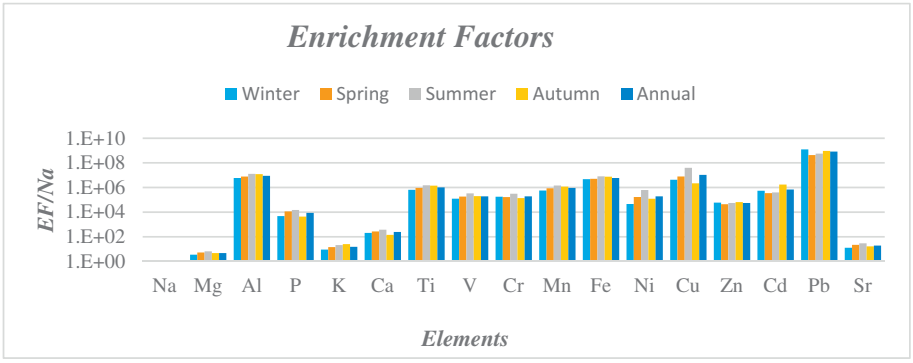

Fig. 6. Enrichment factors of metal elements for different seasons.

lanthanides or rare earth elements (REEs) (Sc, Y, Ce, La, Nd, Pr, Sm, Gd, Dy) in the study area originate mainly from natural dust of crustal origin since they have EFs < 5 for all seasons (Fig. 6b).

The enrichment factors of the selected trace elements varied similarly for all seasons. Seasonal enrichment is greater in winter for most elements, especially for Sb which shows higher EF values in winter compared to other seasons. This again demonstrates that low air exchange during cold periods causes the accumulation of trace elements in the air in urban Constantine. Low EF values were observed in the summer. Similar results were reported by Fang et al. (2006) with the exception of Cu, Ni and V which showed higher EFs in the summer.

3.5. Inter-species correlations

The Pearson correlation coefficients among the metallic species in PM_{10} collected at the sampling site are summarized in Table 6(a, b). The possible sources can be identified qualitatively from the correlation matrix by analyzing the value that represents the linear correlation coefficient between the elements. Strong correlations for Al were observed with Ti (~1), Ga and Co (0.99), Mn (0.98), Fe (0.98), Li (0.97), Sc (0.92), Rb (0.87), Mg (0.88) and Ba (0.86) (Table 6a), suggesting they were predominantly from crustal sources, which is consistent with the results from their EFs analysis. Aluminum also showed important correlations with lanthanides, La and Nd (0.99), Ce and Yb (0.97), Th (0.94), Pr (0.91), Sr (0.88), Nb (0.81), Gd (0.73) in PM_{10} (Table 6b). Lanthanides can be identified as coming exclusively from crustal sources. Similar results have been reported in a previous study conducted by Hsu et al. (2016). Major elements Al, Ca, Fe, K and Mg exhibited good relationships with correlation coefficients between 0.67 and 0.98. With the exception of Al which is depleted in the environment, Ca, Fe, K and Mg were moderately enriched. These elements can be considered as being mainly from natural sources. The strong correlation (0.83–0.9) involving mainly anthropogenic species (As-Ca) with elements originating mainly from natural sources (Cr, V) suggests

Table 6
Inter-species correlations of the metallic species (bold correlations are significant at the 0.01 level).

(a)

	Al	Ca	Fe	K	Mg	S	P	Li	Sc	Ti	Zn	As	Ba	Ga	Rb	Ni	Cu	V	Cr	Mn	Co	Sn	Pb	W	Be	Cd
Al	**1**																									
Ca	**0.67**	**1**																								
Fe	**0.98**	**0.74**	**1**																							
K	**0.80**	**0.72**	**0.81**	**1**																						
Mg	**0.88**	**0.86**	**0.89**	**0.83**	**1**																					
S	**0.52**	**0.75**	**0.59**	**0.66**	**0.71**	**1**																				
P	**0.47**	**0.76**	**0.53**	**0.78**	**0.66**	**0.72**	**1**																			
Li	**0.97**	**0.79**	**0.96**	**0.86**	**0.94**	**0.64**	**0.59**	**1**																		
Sc	**0.92**	**0.45**	**0.88**	**0.66**	**0.76**	0.29	0.27	**0.85**	**1**																	
Ti	**1,00**	**0.66**	**0.97**	**0.79**	**0.87**	**0.52**	0.46	**0.96**	**0.93**	**1**																
Zn	**0.34**	**0.61**	0.47	**0.55**	**0.50**	**0.61**	**0.66**	0.43	0.23	0.33	**1**															
As	**0.66**	**0.90**	**0.74**	**0.74**	**0.82**	**0.80**	**0.73**	**0.76**	0.46	**0.63**	**0.71**	**1**														
Ba	**0.86**	**0.83**	**0.93**	**0.74**	**0.86**	**0.72**	**0.59**	**0.90**	**0.70**	**0.86**	**0.56**	**0.82**	**1**													
Ga	**0.99**	**0.66**	**0.96**	**0.80**	**0.86**	**0.50**	0.47	**0.96**	**0.92**	**0.98**	0.34	**0.65**	**0.85**	**1**												
Rb	**0.87**	**0.63**	**0.86**	**0.80**	**0.79**	**0.52**	0.49	**0.87**	**0.77**	**0.87**	0.43	**0.64**	**0.82**	**0.86**	**1**											
Ni	0.32	**0.34**	0.27	0.32	0.37	0.49	0.42	0.37	0.12	0.33	0.01	0.26	0.36	0.31	0.36	**1**										
Cu	0.21	**0.33**	0.22	0.23	0.26	0.48	0.35	0.26	0	0.21	0.06	0.36	0.36	0.18	0.24	**0.57**	**1**									
V	0.69	**0.82**	**0.73**	**0.83**	**0.82**	**0.90**	**0.80**	**0.78**	0.49	**0.68**	**0.62**	**0.85**	**0.77**	**0.67**	**0.66**	**0.50**	0.41	**1**								
Cr	**0.61**	**0.85**	**0.70**	**0.75**	**0.77**	**0.78**	**0.82**	**0.71**	0.42	**0.59**	**0.72**	**0.90**	**0.76**	**0.60**	**0.61**	0.34	0.32	**0.86**	**1**							
Mn	**0.98**	**0.73**	**0.97**	**0.83**	**0.91**	**0.61**	**0.57**	**0.98**	**0.87**	**0.98**	0.41	**0.71**	**0.91**	**0.96**	**0.88**	0.40	0.29	**0.76**	**0.67**	**1**						
Co	**0.99**	**0.67**	**0.96**	**0.81**	**0.87**	**0.50**	**0.50**	**0.96**	**0.92**	**0.98**	0.36	**0.66**	**0.85**	**1.00**	**0.86**	0.31	0.18	**0.68**	**0.62**	**0.97**	**1**					
Sn	0.37	**0.66**	**0.52**	0.41	0.48	**0.61**	**0.52**	0.45	0.19	0.35	**0.66**	**0.71**	**0.67**	0.38	0.32	0.03	0.16	**0.56**	**0.67**	0.44	0.38	**1**				
Pb	0.17	0.24	0.28	0.08	0.12	0.16	0.08	0.17	0.14	0.15	0.41	0.36	0.39	0.2	0.1	−0.37	−0.17	0.07	0.22	0.17	0.18	**0.69**	**1**			
W	−0.05	0.02	0	0.14	−0.02	0.02	0.01	−0.04	0.01	−0.06	0.21	0.09	0.01	−0.04	0.02	−0.38	−0.27	0.09	0.16	−0.06	−0.05	0.14	0.22	**1**		
Be	−0.14	0.01	−0.05	−0.12	−0.1	0	0.02	−0.1	−0.05	−0.16	0.40	0.17	0	−0.08	−0.07	−0.47	−0.31	−0.02	0.17	−0.14	−0.09	0.32	**0.55**	0.42	**1**	
Cd	−0.01	−0.06	0.01	0.18	−0.05	−0.07	−0.01	−0.03	0.05	−0.02	0.07	0	−0.06	0.01	−0.04	−0.41	−0.29	0.03	0.02	−0.02	0	0.29	0.21	**0.58**	0.15	**1**

(b)

	Al	Sr	Y	Zr	Nb	Cs	Tl	La	Ce	Pr	Nd	Sm	Gd	Dy	Hf	Ta	Th	U
Al	**1**																	
Sr	**0.88**	**1**																
Yb	**0.97**	**0.86**	**1**															
Zr	**0.63**	**0.65**	**0.56**	**1**														
Nb	**0.81**	**0.78**	**0.69**	**0.72**	**1**													
Cs	−0.15	−0.18	−0.1	−0.36	−0.18	**1**												
Tl	−0.08	−0.07	−0.07	−0.07	0	**0.65**	**1**											
La	**0.99**	**0.84**	**0.98**	**0.60**	**0.73**	−0.14		**1**										
Ce	**0.97**	**0.82**	**0.96**	**0.60**	**0.71**	−0.14	−0.1	**0.98**	**1**									
Pr	**0.91**	**0.75**	**0.90**	**0.54**	**0.79**	0.06	0.01	**0.91**	**0.88**	**1**								
Nd	**0.99**	**0.84**	**0.98**	**0.60**	**0.76**	−0.13	−0.1	**1**	**0.98**	**0.92**	**1**							
Sm	**0.63**	0.41	**0.6**	0.034	0.34	0.13	−0.04	**0.67**	**0.69**	**0.68**	**0.67**	**1**						
Gd	**0.73**	**0.52**	**0.79**	0.30	0.40	0.2	−0.01	**0.79**	**0.78**	**0.81**	**0.79**	**0.94**	**1**					
Dy	**0.59**	0.41	**0.66**	0.2	0.26	0.30	0.02	**0.64**	**0.65**	**0.68**	**0.64**	**0.94**	**0.97**	**1**				
Hf	**0.62**	**0.60**	**0.56**	**0.97**	**0.64**	−0.25	−0.08	**0.59**	**0.60**	**0.53**	**0.60**	0.43	0.39	0.31	**1**			
Ta	0.40	0.38	0.38	0.16	0.42	0.2	0.1	0.36	0.38	**0.54**	0.39	**0.60**	**0.59**	**0.64**	0.16	**1**		
Th	**0.94**	**0.76**	**0.95**	**0.44**	**0.65**	0.04	−0.05	**0.95**	**0.93**	**0.91**	**0.95**	**0.70**	**0.84**	**0.72**	0.46	0.46	**1**	
U	**0.50**	**0.50**	**0.51**	0.14	0.2	0.19	0.01	**0.50**	0.47	0.40	0.48	0.23	0.40	0.39	0.19	0.11	**0.57**	**1**

resuspension of traffic-related road dust matter. Elements Ga, Co, Fe, Li, Mn, Ti, Ba and Mg exhibited good correlations (0.85–1) and since they are enriched in the environment, they can be related to natural sources (Table 6a). The composition of road dust has been found to be dominated by elements typically associated with crustal materials (Thorpe and Harrison, 2008). This demonstrates the difficulty in separating road dusts from crustal materials as their compositions may often be quite similar.

The pair V-S (0.9) could be due to fuel oil combustion in diesel vehicles. However, there is no apparent correlation between all elements and Na indicating that sodium was associated only with marine sources. The poor correlation found between Ca and Na ($r = 0.22$) implies that Ca could originate from other sources described in Section 3.4.1. Good correlations were observed for the pairs Zn-As (0.71), Zn-Cr (0.72) and Zn-V (0.62) (Table 6a). A possible source of Zn, As, Cr and V was the foundry and metal processing plant located 3.5 km south of the sampling site (Pey et al., 2013a). Other possible common sources include traffic emissions such as exhaust emissions, brake wear, tyre wear (Wahlin et al., 2006; Amato et al., 2009a; Yatkin and Bayram, 2008). Elemental pairs Zn-Sn (0.66), Zn-Ca (0.61), Zn-K (0.55), Zn-Mg (0.50), Zn-S (0.61) and Zn-P (0.66) are slightly correlated, and because of their high EFs, may be attributed mainly to anthropogenic sources such as traffic emissions including exhaust gases, brake and tyre wear (Amato et al., 2009a), industrial emissions (cement and brick factories) and the resuspension of road dust. When Zn is associated with Ca, S, P, V and Cr, Querol et al. (2004) suggest traffic emissions as the main source. When Zn is associated with Sn and As, these elements are related to non-exhaust emissions due to the degradation of tires and brakes wear, according to Minguillón et al. (2012) and to the corrosion of metal elements, when Zn is associated with Cr. In addition, Cr and V were well correlated ($r = 0.86$), suggesting a possible contribution of fuel oil combustion (Pey et al., 2013b). For Beryllium the highest correlation found, although not particularly strong, was with lead ($r = 0.55$) (Table 6a). A significant proportion of beryllium (Goddard et al., 2016), zinc (Minguillón et al., 2012) and tin (Megido et al., 2016) emissions are attributed to road transport combustion of DERV (diesel oil for road vehicles). There is no correlation between Cd and the others elements, except with W ($r = 0.58$) which reveals that they possibly originated from metallurgical processes (Von Schneidemesser et al., 2010; Zheng et al., 2017).

No good correlation was found between Cu and the other elements. A slight correlation was observed with Ni ($r = 0.57$) (Table 6a). According to Von Uexkull et al. (2005), Ni and Cu were found to be emitted from dust of lining material, which is different from the chemical composition of the brake dust.

3.6. Elemental ratios and source identification

Elemental ratios were often used as diagnostic tools to estimate the profiles of possible sources (Vousta et al., 2002), the origin of air masses (Cheng et al., 2000) and local source fingerprints (Prati et al., 2000; Arditsoglou and Samara, 2005).

The mean values and the range of selected elemental ratios of the area of Zouaghi in Constantine are presented in Table 7 along with literature values for PM_{10}.

Several studies have demonstrated that Cu and Sb may be used as tracers of brake wear in the urban environment (Dongarrà et al., 2007, 2009). A number of authors have found similar Cu/Sb ratios because of significant correlations between Sb and Cu. Sternbeck et al. (2002) found that Cu and Sb are released by brake wear and linings and proposed a Cu/Sb ratio of 4.6 ± 2.3. Dongarrà et al. (2007) reported a ratio in the range 4.2–4.5 and a high significant correlation between Cu and Sb ($r = 0.85$). In a later work, Dongarrà et al. (2009) measured a ratio in the range 3.3–4.9 while a Cu/Sb of ~5 was calculated by Arditsoglou and Samara (2005) for a site dominated by road traffic sources in Kosovo. Such ratios are markedly different from the crustal ratio of around 125 (McLennan, 2001). Brake linings are the source of Sb, since Sb_2S_3 is actually used in many brake linings (Sternbeck et al., 2002). In contrast to these findings, no correlation was found between Cu and Sb in our dataset (Table 6a), and the average Cu/Sb ratio was 20.2 which far exceeds the values reported above. Such findings point out to different sources at our site as Sb and Cu do not always go together in brake linings (Sternbeck et al., 2002). In a chemical profiling study of urban road dust at five main roads of the city of Oporto and in an urban road tunnel in the city of Braga, north of Portugal, Alves et al. (2018) obtained Cu/Sb ratios between 4.8 and 18.9. Cu/Sb ratios > 10 could also be related to metallurgical activities (Thorpe and Harrison, 2008).

Ca/Al ratio had been used as a good marker for the relative influence of the long-transport dust and the locally generated aerosols (Wang et al., 2006). Different values of Ca/Al ratio were observed in Hong Kong as the Ca/Al ratio of 17.32 in cement plant samples was the highest, followed by paved road dust (1.19) (Ho et al., 2003). Similar results were reported by Kong et al. (2011) in which the Ca/Al ratio values were 6.30, 4, 1.29 and 0.84, in cement plant samples, construction dust, paved road dust and soil dust respectively. Another study in California showed similar Ca/Al values between paved road dust (0.45) and construction dust (0.42) (Chow et al., 2003). However, the Ca/Al ratio from the UCC was significantly lower than that of 5.77 recorded at the urban monitoring site of Zouaghi. The latter was similar to ratios in cement plant samples and construction dust reported by Kong et al. (2011). One can assume that Ca originated from the construction site close to the sampling site.

Kong et al. (2011) suggested that the Zn/Pb ratio in PM_{10} in the range (0.03–4.4) might represent vehicle emissions. In the present study, the Zn/Pb ratio was 0.11, as shown in Table 6, while a higher value of 8.4 indicate possible influence of a pyrometallurgical process such as scrap metal incineration (Arditsoglou and Samara, 2005). A very low Cd/Pb ratio (0.028) was observed during our sampling period. High Pb concentration from leaded gasoline may therefore lead to low Cd/Pb and Zn/Pb ratios (Cheng et al., 2011).

The La/Ce ratio in ambient particulate matter has often been used as an indicator of La emissions from the fluid catalytic converter (FCC) systems of refineries (Morishita et al., 2006; Pandolfi et al., 2011), whereby La/Ce ratio can reach up to 5. Similarly, La/Ce ratios at two sites in the Bay of Algeciras in Spain were in the ranges 1.1–1.3 and 1.4–1.7 respectively (Pandolfi et al., 2011). Moreno et al. (2010b) have found that La/Ce > 1 was an indicator of anthropogenic source such as refineries. The mean La/Ce ratio in the present study was 0.492, which is typical of natural crustal composition (around 0.5–0.6) (Pandolfi et al., 2011).

The influence of industrial activities was further confirmed by comparing the V/Ni ratio in this study (1.5) with the same ratio in road dust within an industrial area (1.6) reported by Bosco et al. (2005) and the low V/Ni ratio (< 2) suggested by Moreno et al. (2010a) reflecting the presence of enriched Ni due to the metallurgical plant emissions.

3.7. Principal component analysis

Using PCA, it is possible to simplify the interpretation of complex systems and to reduce the set of variables to a few ones, called principal components (PC_s). Principal component analysis was performed on PM_{10} data sets (64 samples and 48 variables) for a period of one year with varimax rotation. The factors were extracted on the basis of two criteria: first, the cumulative percentage of variance explained by each factor was > 80% and, second, the eigenvalue explained by each factor was > 1. The factor loading, after varimax rotation using the PCA model identified five sources, explaining about 88% of total variance. The matrices of loads found with the PCA are reported in Table 8. The first factor, accounting for 47% of the total variance, presents the highest loading for elements which are dominantly made up of typical soil components (Y, Nd, Th, La, Sc, Ce, Ti, Al, Ga, Co, Pr, Gd, Fe, Mn, Li,

Table 7
Comparison of elemental ratios of urban dust in Constantine and in other studies.

Site	Type	Cu/Sb	Ca/Al	Zn/Pb	La/Ce	V/Ni	Study
Gothenburg,Sweden	Brake wear	4.6 ± 2.3					Sternbeck et al. (2002)
Palermo, Italy	Brake wear and linings	4.2–4.5					Dongarrà et al. (2007)
Catania, Italy	Brake wear	3.3–4.9					Dongarrà et al. (2009)
Hong Kong	Cement plant		17.32				Ho et al. (2003)
	Paved road dust		1.19				
Fushun-a, China	Cement plant		6.30				Kong et al. (2011)
	Construction dust		4				
	Paved road dust		1.29				
	Soil dust		0.84				
	Automotive emissions			0.03–4.4			
California, USA	Paved road dust		0.45				Chow et al. (2003)
	Construction dust		0.42				
Kosovo, Yugoslavia	Scrap metal incineration			8.4			Arditsoglou and Samara (2005)
Bay of Algeciras, Spain	Refinery plant				1.1–1.3		Pandolfi et al. (2011)
					1.4–1.7		
Atlantic Mediterranean sea	Refinery plant				> 1		Moreno et al. (2010b)
Gela, Italy	Road dust (industrial site)					1.6	Bosco et al. (2005)
Constantine, Algeria	Metallurgical processes	20.19					Present study
	Construction dust		5.77				
	Vehicle emissions			0.11			
	Crustal source				0.49		
	Road dust (industrial site)					1.5	
Upper continental crust		125	0.37	4.17	0.47	2.43	McLennan (2001)

Table 8
PCA (with varimax rotation) performed on data from the site of Zouaghi in Constantine (15/01/2015–03/02/2016). Elements with factor loadings > 0.50 are emboldened.

PC1		PC2		PC3		PC4	
Crustal		Soil and road dust resuspension		Traffic		Industrial/ metallurgical emissions	
Y	**0.958**	Y	0.217	Pr	0.196	Pr	0.105
Nd	**0.958**	Nd	0.262	Mn	−0.112	Gd	0.331
Th	**0.957**	Th	0.154	Rb	−0.131	Sr	−0.136
La	**0.957**	La	0.246	Sr	−0.111	Ba	−0.105
Sc	**0.956**	Sc	0.108	Mg	−0.105	K	0.242
Ce	**0.950**	Ce	0.215	As	0.132	Be	0.224
Ti	**0.931**	Ti	0.339	S	−0.145	Ni	−0.375
Al	**0.925**	Al	0.358	P	−0.155	W	**0.859**
Ga	**0.922**	Ga	0.350	V	−0.216	Cd	**0.850**
Co	**0.916**	Co	0.363	Zn	0.339		
Pr	**0.909**	Pr	0.256	Sn	0.461		
Gd	**0.888**	Gd	−0.162	Nb	0.202		
Fe	**0.871**	Fe	0.469	Pb	**0.816**		
Mn	**0.864**	Mn	0.468	Be	**0.771**		
Li	**0.838**	Li	**0.517**	Ni	−0.702		
Rb	**0.781**	Rb	0.410	Ge	−0.632		
Sr	**0.727**	Sr	**0.574**	W	0.231		
Ba	**0.702**	Ba	**0.634**	Cd	0.136		
Mg	**0.699**	Mg	**0.631**				
Cr	0.317	Cr	**0.888**				
As	0.378	As	**0.869**				
S	0.215	S	**0.866**				
P	0.167	P	**0.852**				
V	0.393	V	**0.845**				
Ca	0.404	Ca	**0.833**				
Zn	0.107	Zn	**0.769**				
Sn	0.167	Sn	**0.718**				
Nb	**0.615**	Nb	**0.657**				
K	**0.616**	K	**0.627**				
Pb	0.161	Pb	0.237				
Be	−0.158	Be	0.143				
Ni	0.130	Ni	0.383				
Ge	0.364	Ge	0.412				
		W	0.107				
% of variance	47%	27%		8%		6%	

Rb, Sr, Ba, Mg). Many of these elements (e.g. Al, Fe, Ti, Rb, La, Ce, Nd) have often been reported as deriving from Saharan dust outbreaks and could be used as tracers of the influence of the African events (Negral et al., 2008; Viana et al., 2006; Salvador et al., 2004). Long-range transport of Saharan dust is frequently reported in Mediterranean countries (Querol et al., 2008).

The second factor accounts for 27% of the total variance and it is made up of Cr, As, S, P, V, Ca, Zn, Sn, Nb, Ba, Mg, K, Sr, Li. This factor is representative of the resuspension of local soils and road pavement erosion (Amato et al., 2009a). It may represent a mixture of different emission sources. Mineral elements in this group, Li, Sr, Nb, Sr and Ca may derive from urban soil dust resuspension potentially affected by the nearby construction/demolition works which are high emitters of Ca and Sr (Amato et al., 2009a). Although road dust consists primarily of mineral particles, it is also enriched in heavy metals and metalloids (Amato et al., 2009b). Vehicle brake pad wear leads to the deposition of metal-rich particles. Brake pads are commonly filled with $BaSO_4$, while Sn sulfides are often added as lubricants and Zn is normally used to improve friction (Iijima et al., 2007). Road dust also includes secondary sulfate formed by the photochemical oxidation of sulphur in the atmosphere and particles rich in Zn and Sn which are tracers of brake wear and ultimately of traffic related dust resuspension (Amato et al., 2010; Pey et al., 2010). These elements, initially emitted by breaks are progressively accumulated on roads, particularly after long periods of dry weather and resuspended by vehicle traffic together with crustal dust particles and road wear material (Belis et al., 2013). The continuous resuspension of the urban road dust by vehicular traffic introduces into the atmosphere significant concentrations of these elements (Pey et al., 2010).

The third factor explains 8% of the variance and reflects the influence of traffic emissions. It is mainly made up of Pb. Several previous studies have identified industrial activities as the dominant Pb source. Since lead additives have been phased out around the world following the introduction of legislation imposing the use of unleaded fuel in the European countries from 1 January 2000, leaded gasoline is no longer cited as a potential source of Pb pollution (Pey et al., 2010; Alastuey et al., 2006). Therefore, Pb emissions from traffic have been significantly reduced (Enamorado-Baez et al., 2015). However, leaded gasoline is still used in Algeria (Terrouche et al., 2015). Lead can

therefore be considered as a tracer of vehicle exhaust (Singh and Sharma, 2012). As for Be, a major source of emission is the combustion of fuel oil (Goddard et al., 2016). The share of the diesel fleet in Algeria represents > 60% (Naidja et al., 2018). Beryllium can therefore be considered as a tracer of vehicle traffic. The fourth factor represents 6% of the variance and its tracers are Cd and W. Cadmium has been identified in connection with emissions from industrial metallurgical processes (Von Schneidemesser et al., 2010). Tungsten is mainly used in metal processing (Koutsospyros et al., 2006; Zheng et al., 2017) and in alloys which are used in different welding and metal-cutting applications (EPA, 2017). A possible metallurgical origin for this source cannot be excluded. These elements may be considered as tracers of industrial activities and especially of the mechanical industry located at Oued Hmimime in Constantine. The urban area of Zouaghi in Constantine is affected by two main sources which contribute largely to PM_{10} aerosols: (1) crustal elements originated mainly from African dust events and natural resuspension of semi-arid soils because of the relative proximity of the Sahara and (2) resuspension of road dust affected by demolition and construction works and which accumulates on roads because of the scarcity of precipitation during long periods throughout the year (Querol et al., 2008).

4. Conclusions

An average PM_{10} level of 55.7 $\mu g/m^3$ was observed at an urban area in the city of Constantine between 15 January 2015 and 03 February 2016. It was comparable to PM_{10} levels observed at different sites in the Mediterranean and North African regions. Although this level may be considered as relatively high when compared with WHO or European air quality standards, it remains below the Algerian annual limit of 80 $\mu g/m^3$. Daily PM_{10} levels were influenced by African dust outbreaks, as suggested by the analysis of HYSPLIT back trajectories and BSC-DREAM arerosol maps.

Crustal elements Ca, Al, S, Fe and Na were the dominant components in PM_{10} and anthropogenic metals Pb, Cu, Zn, Ba and Mn had the highest concentrations among the measured trace metals. The influence of precipitation was shown to be significant as it reflected the remarkable decrease of PM_{10} and trace elements levels in rainy days.

Crustal enrichment factor calculations showed that elements Pb, Sb, Cd, Bi, Cu, As, Zn, Sn, and Ca had EF values higher than 100 which confers upon them an anthropogenic character. Elements including Ba, Cs, Cr, Ni, V, Co and Mn were not enriched and were thus, influenced both by natural sources and road dust resuspension which included particles of anthropogenic nature such as tire and brake fragments as well as material from abrasion of pavement and mechanical parts of road vehicles.

Cu/Sb, Ca/Al, Zn/Pb, La/Ce, and V/Ni ratios can be considered as markers of metallurgical processes, construction works, vehicle emissions, soil dust and road dust respectively.

Source apportionment was performed by factor analysis using PCA (varimax rotated factor matrix method) in SPSS 20. The statistical analysis by PCA of the PM_{10} data from the urban site in the city of Constantine allowed to identify four main emission sources. The latter were crustal sources (including REEs), soil dust resuspension (both road/city and soil dust), traffic emissions and industrial metallurgical processes. PCA results revealed that crustal materials especially Saharan dust and resuspended dust were important sources of trace elements in PM_{10} at the study site. Evidence of adverse health effects of both desert and non-desert sources strengthens the need to control for anthropogenic sources, by reducing anthropogenic emissions and population exposure especially on desert dust advection days.

The present study focused on the identification of principal sources affecting the ambient air of Constantine. Further research is needed to apportion the possible sources of PM_{10} over the study period.

Acknowledgements

The authors gratefully acknowledge the provision of the PM_{10} quartz fiber filters and sample analysis support received from Professor Xavier Querol of the Institute of Environmental Assessment and Water Research (IDAEA-CSIC, Barcelona, Spain). An acknowledgment is also given for the comments made by the editor and anonymous reviewers for helpful comments and corrections to improve the quality of this manuscript.

References

Alastuey, A., Querol, X., Plana, F., Viana, M., Ruiz, C.R., Sánchez de la Campa, A., de la Rosa, J., Mantilla, E., dos Santos, S.G., 2006. Identification and chemical characterization of industrial particulate matter sources in Southwest Spain. Air and Waste Manage. Assoc. 56, 993–1006. https://doi.org/10.1080/10473289.2006.10464502.

Aleksandropoulou, V., Lazaridis, M., 2012. Identification of the Influence of African Dust on PM10 Concentrations at the Athens Air Quality Monitoring Network during the period 2001–2010. Aerosol Air Qual. Res. 13 (5), 1492–1503. https://doi.org/10.4209/aaqr.2012.12.0363.

Alharbi, B., Mujtaba Shareef, M., Husain, T., 2015. Study of chemical characteristics of particulate matter concentrations in Riyadh, Saudi Arabia. Atmos. Pollut. Res. 6, 88–98. https://doi.org/10.5094/APR.2015.011.

Ali-Khodja, H., Belaala, A., Demmane-Debbih, W., Habbas, B., Boumagoura, N., 2008. Air quality and deposition of trace elements in Didouche Mourad, Algeria. Environ. Monit. Assess. 138, 219–231. https://doi.org/10.1007/s10661-007-9792-1.

Alleman, L., Lamaison, L., Perdrix, E., Robache, A., Galloo, J., 2010. PM10 metal concentrations and source identification using positive matrix factorization and wind sectoring in a French industrial zone. Atmos. Res. 96, 612–625. https://doi.org/10.1016/j.atmosres.2010.02.008.

Al-Momani, I., Daradkeh, A., Haj-Hussein, A., Yousef, Y., Jaradat, Q., Momani, K., 2005. Trace elements in daily collected aerosols in Al-Hashimya, Central Jordan. Atmos. Res. 73, 87–100. https://doi.org/10.1016/j.atmosres.2003.09.009.

Alves, C.A., Evtyugina, M., Vicente, A.M.P., Vicente, E.D., Nunes, T.V., Silva, P.M.A., Duarte, M.A.C., Pio, C.A., Amato, F., Querol, X., 2018. Chemical profiling of PM10 from urban road dust. Sci. Total Environ. 634, 41–51. https://doi.org/10.1016/j.scitotenv.2018.03.338.

Amato, F., Pandolfi, M., Viana, M., Querol, X., Alastuey, A., Moreno, T., 2009a. Spatial and chemical patterns of PM10 in road dust deposited in urban environment. Atmos. Environ. 43, 1650–1659. https://doi.org/10.1016/j.atmosenv.2008.12.009.

Amato, F., Pandolfi, M., Escrig, A., Querol, X., Alastuey, A., Pey, J., Pérez, N., Hopke, P., 2009b. Quantifying road dust resuspension in urban environment by Multilinear Engine: a comparison with PMF2. Atmos. Environ. 43, 2770–2780. https://doi.org/10.1016/j.atmosenv.2009.02.039.

Amato, F., Nava, S., Lucarelli, F., Querol, X., Alastuey, A., Baldasano, J.M., Pandolfi, M., 2010. A comprehensive assessment of PM emissions from paved roads: real-world emission factors and intense street cleaning trials. Sci. Total Environ. 408, 4309–4318. https://doi.org/10.1016/j.scitotenv.2010.06.008.

Amato, F., Viana, M., Richard, A., Furger, M., Prévot, A., Nava, S., Lucarelli, F., Bukowiecki, N., Alastuey, A., Reche, C., Moreno, T., Pandolfi, M., Pey, J., Querol, X., 2011. Size and time-resolved roadside enrichment of atmospheric particulate pollutants. Atmos. Chem. Phys. 11, 2917–2931. https://doi.org/10.5194/acp-11-2917-2011.

Arditsoglou, A., Samara, C., 2005. Levels of total suspended particulate matter and major trace elements in Kosovo: a source identification and apportionment study. Chemosphere 59, 669–678. https://doi.org/10.1016/j.chemosphere.2004.10.056.

Belis, C.A., Karagulian, F., Larsen, B.R., Hopke, P.K., 2013. Critical review and meta-analysis of ambient particulate matter source apportionment using receptor models in Europe. Atmos. Environ. 69, 94–108. https://doi.org/10.1016/j.atmosenv.2012.11.009.

Belzile, N., Chen, Y.-W., Filella, M., 2011. Human exposure to antimony: I. Sources. Crit. Rev. Environ. Sci. Technol. 41, 1309–1373. https://doi.org/10.1080/10643381003608227.

Benaissa, F., Maesano, C., Alkama, R., Annesi-Maesano, I., 2016. Short-term health impact assessment of urban PM10 in Bejaia City (Algeria). Can. Respir. J. 1–6. https://doi.org/10.1155/2016/8209485.

Bosco, M.L., Varrica, D., Dongarrà, G., 2005. Case study: inorganic pollutants associated with particulate matter from an area near a petrochemical plant. Environ. Res. 99, 18–30. https://doi.org/10.1016/j.envres.2004.09.011.

Bouchlaghem, K., Nsom, B., 2012. Effect of atmospheric pollutants on the air quality in Tunisia. Sci. World J. 1–8. https://doi.org/10.1100/2012/863528.

Bouhila, F., Mouzai, M., Azli, T., Nedjar, A., Mazouzi, C., Zergoug, Z., Boukhadra, D., Chegrouche, S., Lounici, H., 2015. Investigation of aerosol trace element concentrations nearby Algiers for environmental monitoring using instrumental neutron activation analysis. Atmos. Res. 1-28. https://doi.org/10.1016/j.atmosres.2015.06.013.

Bourbia, F., Boucheriba, F., 2010. Impact of street design on urban microclimate for semi arid climate (Constantine). Renew. Energy 35, 343–347. https://doi.org/10.1016/j.renene.2009.07.017.

Bozkurt, Z., Gaga, E.O., Taşpınar, F., Arı, A., Pekey, B., Pekey, H., Döğeroğlu, T., Üzmez, Ö.Ö., 2018. Atmospheric ambient trace element concentrations of PM10 at urban and sub-urban sites: source apportionment and health risk estimation. Environ. Monit.

Assess. 190 (168), 1–17. https://doi.org/10.1007/s10661-018-6517-6.
Budhavant, K., Safai, P., Rao, P., 2015. Sources and elemental composition of summer aerosols in the Larsemann Hills (Antarctica). Environ. Sci. Pollut. Res. 22, 2041–2050. https://doi.org/10.1007/s11356-014-3452-0.
Cesari, D., Contini, D., Genga, A., Siciliano, M., Elefante, C., Baglivi, F., Daniele, L., 2012. Analysis of raw soils and their re-suspended PM_{10} fractions: characterisation of source profiles and enrichment factors. Appl. Geochem. 27, 1238–1246. https://doi.org/10.1016/j.apgeochem.2012.02.029.
Cheng, M.C., You, C.F., Lin, F.J., Huang, K.F., Chung, C.H., 2011. Sources of Cu, Zn, Cd and Pb in rainwater at a subtropical islet offshore northern Taiwan. Atmos. Environ. 45, 1919–1928. https://doi.org/10.1016/j.atmosenv.2011.01.034.
Cheng, X., Huang, Y., Zhang, S.-P., Ni, S.-J, Long, Z.-J., 2018. Characteristics, sources, and health risk assessment of trace elements in PM10 at an urban site in Chengdu, Southwest China. Aerosol Air Qual. Res. 18, 357–370. https://doi.org/10.4209/aaqr.2017.03.0112.
Cheng, Z.L., Lam, K.S., Chan, L.Y., Wang, T., Cheng, K.K., 2000. Chemical characteristics of aerosols at coastal station in Hong Kong. I. Seasonal variation of major ions, halogens and mineral dusts between 1995 and 1996. Atmos. Environ. 34, 2771–2783. https://doi.org/10.1016/S1352-2310(99)00343-X.
Chow, J.C., Watson, J.G., Ashbaugh, L.L., Magliano, K.L., 2003. Similarities and differences in PM10 chemical source profiles for geological dust from the San Joaquin Valley, California. Atmos. Environ. 37, 1317–1340. https://doi.org/10.1016/S1352-2310(02)01021-X.
Christian, T., Yokelson, R., Cardenas, B., Molina, L., Engling, G., Hsu, S.-C., 2010. Trace gas and particle emissions from domestic and industrial biofuel use and garbage burning in Central Mexico. Atmos. Chem. Phys. 10, 565–584. https://doi.org/10.5194/acp-10-565-2010.
Dai, Q.-L., Bi, X.-H., Wu, J.-H., Zhang, Y.-F., Wang, J., Xu, H., Yao, L., Jiao, L., Feng, Y.-C., 2015. Characterization and source identification of heavy metals in ambient PM_{10} and background site. Aerosol Air Qual. Res. 15, 875–887. https://doi.org/10.4209/aaqr.2014.09.0226.
Dall'Osto, M., Querol, X., Amato, F., Karanasiou, A., Lucarelli, F., Nava, S., Calzolai, G., Chiari, M., 2012. Hourly elemental concentrations in $PM_{2.5}$ aerosols sampled simultaneously at urban background and road site. Atmospheric Chemistry and Physics. Discuss. 12, 20135–20180. https://doi.org/10.5194/acpd-12-20135-2012.
Dongarrà, G., Manno, E., Varrica, D., Vultaggio, M., 2007. Mass levels, crustal component and trace elements in PM10 in Palermo, Italy. Atmos. Environ. 41, 7977–7986. https://doi.org/10.1016/j.atmosenv.2007.09.015.
Dongarrà, G., Manno, E., Varrica, D., 2009. Possible markers of traffic-related emissions. Environment Monitoring Assessment 154, 117–125. https://doi.org/10.1007/s10661-008-0382-7.
Draxler, R.R., Hess, G.D., 1998. An overviewof the HYSPLIT_4 modelling system for trajectories,dispersionand deposition. Aust. Meteorol. Mag. 47, 295–308.
Elhadi, R.E., Abdullah, A.M., Abdullah, A.H., Ash'aari, Z.H., Kura, N.U., Gumel, D.Y., Adamu, A., 2017. Source identification of heavy metals in particulate matter (PM_{10}) in a Malaysian traffic area using multivariate techniques. Polish Journal Environmental Studies 26 (6), 2523–2532. https://doi.org/10.15244/pjoes/69941.
Elichegaray, C., Bouallala, S., Maitre, A., Ba, M., 2010. État et évolution de la pollution atmosphérique development and current status of atmospheric pollution. Revue Française d'Allergologie 50, 381–393. https://doi.org/10.1016/j.reval.2009.08.003.
Enamorado-Baez, S., Gomez-Guzma, J., Chamizo, E., Abril, J., 2015. Levels of 25 trace elements in high-volume air filter samples from Seville (2001 − 2002): sources, enrichment factors and temporal variations. Atmos. Res. 155, 118–129. https://doi.org/10.1016/j.atmosres.2014.12.005.
EPA, 2017. Technical Fact Sheet – Tungsten.
Fang, G.-C., Wu, Y.-S., Chang, S.-Y., Huang, S.-H., Rau, J.-Y., 2006. Size distributions of ambient air particles and enrichment factor analyses of metallic elements at Taichung Harbor near the Taiwan Strait. Atmos. Res. 81, 320–333. https://doi.org/10.1016/j.atmosres.2006.01.007.
Feng, X.-D., Dang, Z., Huang, W.-L., Yang, C., 2009. Chemical speciation of fine particle bound trace metals. Int. J. Environ. Sci. Technol. 6 (3), 337–346. https://doi.org/10.1007/BF03326071.
Filella, M., Williams, P.A., Belzile, N., 2009. Antimony in the environment: knowns and unknowns. Environ. Chem. 6, 95–105. https://doi.org/10.1071/EN09007.
Gao, Y., Nelson, E.D., Field, M.P., Ding, Q., Li, H., Sherrell, R.M., Gigliotti, C.L., Van Ry, D.A., Glenn, T.R., Eisenreich, S.J., 2002. Characterization of atmospheric trace elements on $PM_{2.5}$ particulate matter over the New York–New Jersey harbor estuary. Atmos. Environ. 36, 1077–1086. https://doi.org/10.1016/S1352-2310(01)00381-8.
Garcia, M.A., Sánchez, M.L., de los Ríos, A., Pérez, I.A., Pardo, N., Fernández-Duque, B., 2018. Analysis of PM_{10} and $PM_{2.5}$ concentrations in an urban atmosphere in Northern Spain. Arch. Environ. Contam. Toxicol. 76 (2), 331–345. https://doi.org/10.1007/s00244-018-0581-3.
Genga, A.B., 2012. SEM-EDS investigation on PM10 data collected in Central Italy: principal component analysis and hierarchical cluster analysis. Chemistry Central Journal 6 (2), 2–15. https://doi.org/10.1186/1752-153X-6-S2-S3.
Goddard, S.L., Brown, R.J., Ghatora, B.K., 2016. Determination of beryllium concentrations in UK ambient air. Atmos. Environ. 147, 320–329. https://doi.org/10.1016/j.atmosenv.2016.10.018.
Hieu, N.T., Lee, B.-K., 2010. Characteristics of particulate matter and metals in the ambient air from a residential area in the largest industrial city in Korea. Atmos. Res. 98, 526–537. https://doi.org/10.1016/j.atmosres.2010.08.019.
Ho, K.F., Lee, S.C., Chow, J.C., Watson, J.G., 2003. Characterization of PM10 and PM2.5 source profiles for fugitive dust in Hong Kong. Atmos. Environ. 37, 1023–1032. https://doi.org/10.1016/S1352-2310(02)01028-2.
Hsu, C., Chiang, H., Lin, S., Chen, M., Lin, T., Chen, Y., 2016. Elemental characterization and source apportionment of PM_{10} and $PM_{2.5}$ in the western coastal area of central Taiwan. Sci. Total Environ. 541, 1139–1150. https://doi.org/10.1016/j.scitotenv.2015.09.122.
Huang, L., Wang, K., Yuan, C.-S., Wang, G., 2010. Study on the seasonal variation and source apportionment of PM_{10} in Harbin China. Aerosol Air Qual. Res. 10, 86–93. https://doi.org/10.4209/aaqr.2009.04.0025.
Iijima, A., Sato, K., Yano, K., Tago, H., Kato, M., Kimura, H., Furuta, N., 2007. Particle size and composition distribution analysis of automotive brake abrasion dusts for the evaluation of antimony sources of airborne particulate matter. Atmos. Environ. 41, 4908–4919. https://doi.org/10.1016/j.atmosenv.2007.02.005.
Iijima, A., Sato, K., Fujitani, Y., Fujimori, E., Saito, Y., Tanabe, K., Ohara, T., Kozawa, K., Furuta, N., 2009. Clarification of the predominant emission sources of antimony in airborne particulate matter and estimation of their effects on the atmosphere in Japan. Environment Chemistry 6, 122–132. https://doi.org/10.1071/EN08107.
Kalaiarasan, G., Balakrishnan, R.M., Khaparde, V.V., 2016. Receptor model based source apportionment of PM_{10} in the metropolitan and industrialized areas of Mangalore. Environ. Technol. Innov. 6, 195–203. https://doi.org/10.1016/j.eti.2016.10.002.
Kara, M., Dumanoglu, Y., Altıok, H., Elbir, T., Odabası, M., Bayram, A., 2014. Seasonal and spatial variation of atmospheric trace elemental deposition in the Aliaga industrial region, Turkey. Atmos. Res. 149, 204–216. https://doi.org/10.1016/j.atmosres.2014.06.009.
Karar, K., Gupta, A.K., 2006. Seasonal variations and chemical characterization of ambient PM_{10} at residential and industrial sites of an urban region of Kolkata (Calcutta), India. Atmos. Res. 81, 36–53. https://doi.org/10.1016/j.atmosres.2005.11.003.
Karar, K., Gupta, A.K., 2007. Source apportionment of PM10 at residential and industrial sites of an urban region of Kolkata, India. Atmos. Res. 84, 30–41. https://doi.org/10.1016/j.atmosres.2006.05.001.
Kassomenos, P., Dimitriou, K., Paschalidou, A., 2013. Human health damage caused by particulate matter PM10 and ozone in urban environments: the case of Athens, Greece. Environ. Monit. Assess. 185, 6933–6942. https://doi.org/10.1007/s10661-013-3076-8.
Kemmouche, A., Ali-Khodja, H., Bencharif-Madani, F., López Mahía, P., Querol, X., 2017. Comparative study of bulk and partial digestion methods for airborne PM_{10}-bound elements in a high mineral dust urban site in Constantine, Algeria. International Journal of Environmental Analytical 1–19. https://doi.org/10.1080/03067319.2017.1390088.
Kong, S., Ji, Y., Lu, B., Chen, L., Han, B., Li, Z., Bai, Z., 2011. Characterization of PM10 source profiles for fugitive dust in Fushun-a city famous for coal. Atmos. Environ. 45, 5351–5365. https://doi.org/10.1016/j.atmosenv.2011.06.050.
Koutsospyros, A., Braida, W., Christodoulatos, C., Dermatas, D., Strigul, N., 2006. A review of tungsten: from environmental obscurity to scrutiny. J. Hazard. Mater. 136, 1–19. https://doi.org/10.1016/j.jhazmat.2005.11.007.
Lage, J., Wolterbeek, H., Almeida, S.M., 2016. Contamination of surface soils from a heavy industrial area in the North of Spain. J. Radioanal. Nucl. Chem. 309, 429–437. https://doi.org/10.1007/s10967-016-4757-x.
Laïd, Y., Atek, M., Oudjehane, R., Filleul, L., Baough, L., Zidouni, N., Boughedaoui, M., Tessier, J.-F., 2006. Impact sanitaire de la pollution de l'air par les PM_{10} dans une ville du sud: le cas d'Alger. International Journal of Tuberculosis and Lung Disease 10 (12), 1406–1411.
Lal, R., 2001. Potential of desertification control to sequester carbon and mitigatethe greenhouse effect. Clim. Chang. 51 (1), 35–72. https://doi.org/10.1023/A:1017529816140.
Lim, J., Lee, J., Moon, J., Chung, Y., Kim, K., 2010. Airborne PM10 and metals from multifarious sources in an industrial complex area. Atmos. Res. 96, 53–64. https://doi.org/10.1016/j.atmosres.2009.11.013.
Matassoni, L., Pratesi, G., Centioli, D., Cadoni, F., Malesani, P., Caricchia, A. M., and Di Menno di Bucchianico, A., (2009). Saharan dust episodes in Italy: influence on PM_{10} daily limit value (DLV) exceedances and the related synoptic. J. Environ. Monit.. 11, 1586–1594. doi:https://doi.org/10.1039/B903822A.
McLennan, S., 2001. Relationships between the trace element composition of sedimentary rocks and upper continental crust. Geochemistry.Geophysics. Geosystems journal. 2, 1–24. https://doi.org/10.1029/2000GC000109.
Megido, L., Negral, L., Castrillón, L., Suárez-Peña, B., Fernández-Nava, Y., Marañón, E., 2016. Enrichment factors to assess the anthropogenic influence on PM_{10}. Environ. Sci. Pollut. Res. 1–14. https://doi.org/10.1007/s11356-016-7858-8.
Mijic, Z., Stojic, A., Perisic, M., Rajsic, S., Tasic, M., Radenkovic, M., Joksic, J., 2010. Seasonal variability and source apportionment of metals in the atmospheric deposition in Belgrade. Atmos. Environ. 44, 3630–3673. https://doi.org/10.1016/j.atmosenv.2010.06.045.
Miller-Schulze, J.P., Shafer, M., Schauer, J.J., Heo, J., Solomon, P.A., Lantz, J., Artamonova, M., Chen, B., Imashev, S., Sverdlik, L., Carmichael, G., DeMinter, J., 2015. Seasonal contribution of mineral dust and other major components to particulate matter at two remote sites in Central Asia. Atmos. Environ. 119, 11–20. https://doi.org/10.1016/j.atmosenv.2015.07.011.
Minguillón, M., Querol, X., Baltensperger, U., Prévôt, A., 2012. Fine and coarse PM composition and sources in rural and urban sites in Switzerland: local or regional pollution? Sci. Total Environ. 427-428, 191–202. https://doi.org/10.1016/j.scitotenv.2012.04.030.
Mkoma, S., Maenhaut, W., Chi, X., Wang, W., Raes, N., 2009. Characterisation of PM10 atmospheric aerosols for the wet season 2005 at two sites in East Africa. Atmos. Environ. 43, 631–639. https://doi.org/10.1016/j.atmosenv.2008.10.008.
Mooibroek, D., Staelens, J., Cordell, R., Panteliadis, P., Delaunay, T., Weijers, E., Vercauteren, J., Hoogerbrugge, R., Dijkema, M., Monks, P.S., Roekens, E., 2016. PM10 source apportionment in five north western European cities-outcome of the Joaquin project. In: Harrison, R.M., Hester, R.E. (Eds.), Airborne Particulate Matter: Sources, Atmospheric Processes and Health. The Royal Society of Chemistry, Cambridge, UK, pp. 264–289.

Moreno, T., Querol, X., Alastuey Moreno, T., Querol, X., Alastuey, A., Viana, M., Salvador, P., Sanchez de la Campa, A., Artinano, B., de la Rosa, J., Gibbons, W., 2006. Variations in atmospheric PM trace metal content in Spanish towns: Illustrating the chemical complexity of the inorganic urban aerosol cocktail. Atmos. Environ. 40, 6791–6803. https://doi.org/10.1016/j.atmosenv.2006.05.074.

Moreno, T., Querol, X., Alastuey, A., Amato, F., Pey, J., Pandolfi, M., Kuenzli, N., Bouso, L., Rivera, M., Gibbon, W., 2010. Effects of fireworks events on urban background trace metal aerosol concentrations: is the cocktail worth the show? J. Hazard. Mater. 183, 945–949. https://doi.org/10.1016/j.jhazmat.2010.07.082.

Moreno, T., Querol, X., Alastuey, A., de la Rosa, J., Sánchez de la Campa, A.M., Minguillón, M., Pandolfi, M., González-Castanedo, Y., Monfort, E., Gibbons, W., 2010a. Variations in vanadium, nickel and lanthanoid element concentrations in urban air. Sci. Total Environ. 408, 4569–4579. https://doi.org/10.1016/j.scitotenv.2010.06.016.

Moreno, T., Pérez, N., Querol, X., Amato, F., Alastuey, A., Bhatia, R., Spiro, B., Hanvey, M., Gibbons, W., 2010b. Physicochemical variations in atmospheric aerosols recorded at sea on board the Atlantice Mediterranean 2008 Scholar Ship cruise (PartII): natural versus anthropogenic influences revealed by PM_{10} trace element geochemistry. Atmos. Environ. 44, 2563–2576. https://doi.org/10.1016/j.atmosenv.2010.04.027.

Morishita, M., Keeler, G.J., Kamal, A.S., Wagner, J.G., Harkema, J.R., Rohr, A.C., 2011. Identification of ambient PM2.5 sources and analysis of pollution episodes in Detroit, Michigan using highly time-resolved measurements. Atmos. Environ. 45, 1627–1637. https://doi.org/10.1016/j.atmosenv.2010.09.062.

Morishita, M.K., 2006. Source identification of ambient $PM_{2.5}$ during summer inhalation exposure studies in Detroit, MI. Atmos. Environ. 40, 3823–3834. https://doi.org/10.1016/j.atmosenv.2006.03.005.

Naidja, L., Ali-Khodja, H., Khardi, S., 2018. Sources and levels of particulate matter in North African and Sub-Saharan cities: a literature review. Environ. Sci. Pollut. Res. https://doi.org/10.1007/s11356-018-1715-x.

Negral, L., Moreno-Grau, S., Moreno, J., Querol, X., Viana, M., Alastuey, A., 2008. Natural and anthropogenic contributions to PM10 and PM2.5 in an urban area in the Western Mediterranean Coast. Water Air Soil Pollut. 192, 227–238. https://doi.org/10.1007/s11270-008-9650-y.

Olawoyin, R., Schweitzer, L., Zhang, K., Okareh, O., Slates, K., 2018. Index analysis and human health risk model application for evaluating ambient air-heavy metal contamination in Chemical Valley Sarnia. Ecotoxicol. Environ. Saf. 148, 72–81. https://doi.org/10.1016/j.ecoenv.2017.09.069.

Pacyna, J.M., Pacyna, E.G., 2001. An assessment of global and regional emissions of trace metals to the atmosphere from anthropogenic sources worldwide. Environmental Reivew 9, 269–298.

Padoan, E., Malandrino, M., Giacomino, A., Grosa, M., Lollobrigida, F., Martini, S., Abollino, O., 2016. Spatial distribution and potential sources of trace elements in PM10 monitored in urban and rural sites of Piedmont Region. Chemosphere 145, 495–507. https://doi.org/10.1016/j.chemosphere.2015.11.094.

Pandey, M., Kumar Pandey, A., Mishra, A., Tripathi, B., 2017. Speciation of carcinogenic and non-carcinogenic metals in respirable suspended particulate matter (PM10) in Varanasi, India. Urban Clim. https://doi.org/10.1016/j.uclim.2017.01.004.

Pandolfi, M., Gonzalez-Castanedo, Y., Alastuey, A., de la Rosa, J.D., Mantilla, E., Sanchez de la Campa, A., Querol, X., Pey, J., Amato, F., Moreno, T., 2011. Source apportionment of PM10 and PM2.5 at multiple sites in the strait of Gibraltar by PMF: impact of shipping emissions. Environ. Sci. Pollut. Res. 18, 260–269. https://doi.org/10.1007/s11356-010-0373-4.

Papanastasiou, D.K., Poupkou, A., Katragkou, E., Amiridis, V., Melas, D., Mihalopoulos, N., Basart, S., Perez, C., Baldasano, J.M., 2010. An Assessment of the Efficiency of Dust Regional Modelling to Predict Saharan Dust Transport Episodes. Adv. Meteorol. 2010, 1–9. https://doi.org/10.1155/2010/154368.

Pasha, M.J., Alharbi, B.H., 2015. Characterization of size–fractionated PM10 and associated heavy metals at two semi–arid holy sites during Hajj in Saudi Arabia. Atmospheric Pollution Research 6, 162–172. https://doi.org/10.5094/APR.2015.019.

Pateraki, S., Asimakopoulos, D.N., Flocas, H.A., Maggos, T., Vasilakos, C., 2012. The role of meteorology on different sized aerosol fractions (PM10, PM2.5, PM2.5–10). Sci. Total Environ. 419, 124–135. https://doi.org/10.1016/j.scitotenv.2011.12.064.

Pay, M., Jiménez-Guerrero, P., Jorba, O., Basart, S., Querol, X., Pandolfi, M., Baldasano, J., 2012. Spatio-temporal variability of concentrations and speciation of particulate matter across Spain in the CALIOPE modeling system. Atmos. Environ. 46, 376–396. https://doi.org/10.1016/j.atmosenv.2011.09.049.

Pérez, N., Pey, J., Castillo, S., Viana, M., Alastuey, A., Querol, X., 2008. Interpretation of the variability of levels of regional background aerosols in the Western Mediterranean. Sci. Total Environ. 407, 527–540. https://doi.org/10.1016/j.scitotenv.2008.09.006.

Pey, J., Alastuey, A., Querol, X., Rodriguez, S., 2010. Monitoring of sources and atmospheric processes controlling air quality in an urban Mediterranean environment. Atmos. Environ. 44, 4879–4890. https://doi.org/10.1016/j.atmosenv.2010.08.034.

Pey, J., Alastuey, A., Querol, X., 2013a. PM10 and PM2.5 sources at an insular location in the western Mediterranean by using source apportionment techniques. Sci. Total Environ. 456–457, 267–277. https://doi.org/10.1016/j.scitotenv.2013.03.084.

Pey, J., Pérez, N., Cortés, J., Alastuey, A., Querol, X., 2013b. Chemical fingerprint and impact of shipping emissions over a western Mediterranean metropolis: primary and aged contributions. Sci. Total Environ. 463–464, 497–507. https://doi.org/10.1016/j.scitotenv.2013.06.061.

Pope III, C., Dockery, D., 2006. Health Effects of Fine Particulate Air Pollution: Lines that Connect. J. Air Waste Manag. Assoc. 56, 709–942. https://doi.org/10.1080/10473289.2006.10464485.

Prati, P., Zucchiatti, A., Lucarelli, F., Mando, P.A., 2000. Source apportionment near a steel plant in Genoa (Italy) by continuous aerosol sampling and PIXE analysis. Atmos. Environ. 34, 3148–3157. https://doi.org/10.1016/S1352-2310(99)00421-5.

Prospero, J., Ginoux, P., Torres, O., Nicholson, S., Gill, T., 2002. Environmental characterization of global sources of atmospheric soil dust identified with the nimbus 7total ozone mapping spectrometer (TOMS) absorbing aerosol product. Rev. Geophys. 40 (1), 1–31. https://doi.org/10.1029/2000RG000095.

Querol, X., Alastuey, A., Puicercus, J.A., Mantilla, E., Miro, J.V., Lopez-Soler, A., Plana, F., Artinano, B., 1998. Seasonal evolution of suspended particle around a large coal-fired power station: particulate levels and sources. Atmos. Environ. 32 (11), 1963–1978.

Querol, X., Alastuey, A., Rodriguez, S., Plana, F., Mantilla, E., Ruiz, C.R., 2001. Monitoring of PM10 and PM2.5 around primary particulate anthropogenic emission sources. Atmos. Environ. 35, 845–858. https://doi.org/10.1016/S1352-2310(00)00387-3.

Querol, X., Alastuey, A., Viana, M.M., Rodriguez, S., Artinano, B., Salvador, P., Garcia do Santos, S., Fernandez Patier, R., Ruiz, C.R., de la Rosa, J., Sanchez de la Campa, A., Menendez, M., Gil, J.I., 2004. Speciation and origin of PM10 and PM2.5 in Spain. Aerosol Science 35, 1151–1172. https://doi.org/10.1016/j.jaerosci.2004.04.002.

Querol, X., Zhuang, X., Alastuey, A., Viana, M., Lv, W., Wang, Y., Lopez, A., Zhu, Z., Wei, H., Xu, S., 2006. Speciation and sources of atmospheric aerosols in a highly industrialised emerging mega-city in Central China. J. Environ. Monit. 8, 1049–1059. https://doi.org/10.1039/b608768j.

Querol, X., Pey, J., Minguillon, M. C., Pérez, N., Alastuey, A., Viana, M. M., Castillo, S., Pey, J., Rodrı'guez, S., Artinano, B., Salvador, P., Sa'nchez, M., Garcia Dos Santos, S., Herce Garraleta, M.D., Fernandez-Patier, R., Moreno-Grau, S., Negral, L., Minguillon, M.C., Monfort, E., Sanz, M.J., Palomo-Marin, R., Pinilla-Gil, E., Cuevash, E., de la Rosa, J., Sanchez de la Campa, A., (2008). Spatial and temporal variations in airborne particulate matter (PM10 and PM2.5) across Spain 1999–2005. Atmos. Environ. 42, 3964–3979. doi:https://doi.org/10.1016/j.atmosenv.2006.10.071.

Querol, X., Pey, J., Pandolfi, M., Alastuey, A., Cusack, M., Perez, N., Moreno, T., Viana, M., Mihalopoulos, N., Kallos, G., Kleanthous, S., 2009. African dust contributions to mean ambient PM10 mass-levels across the Mediterranean Basin. Atmos. Environ. 43, 4266–4277. https://doi.org/10.1016/j.atmosenv.2009.06.013.

Rodriguez, S., Querol, X., Alastuey, A., Viana, M., Alarcon, M., Mantilla, E., Ruiz, C., 2004. Comparative PM10–PM2.5 source contribution study at rural, urban and industrial sites during PM episodes in Eastern Spain. Sci. Total Environ. 328, 95–113. https://doi.org/10.1016/S0048-9697(03)00411-X.

Rodrigez, S., Alastuey, A., Alonzo-Perez, S., Querol, X., Cuevas, E., Abreu-Alfonso, J., Viana, M., Pandolfi, M., De la Rosa, J., 2011. Transport of desert dust mixed with North African industrial pollutants in the subtropical Saharan Air Layer. Atmos. Chem. Phys. 11, 8841–8892. https://doi.org/10.5194/acpd-11-8841-2011.

Salvador, P., Artınano, B., Alonso, D.G., Querol, X., Alastuey, A., 2004. Identification and characterisation of sources of PM10 in Madrid (Spain) by statistical methods. Atmos. Environ. 38, 435–447. https://doi.org/10.1016/j.atmosenv.2003.09.070.

Salvador, P., Artíñano, B., Molero, F., Viana, M., Pey, J., Alastuey, A., Querol, X., 2013. African dust contribution to ambient aerosol levels across central Spain: characterization of long-range transport episodes of desert dust. Atmos. Res. 127, 117–129. https://doi.org/10.1016/j.atmosres.2011.12.011.

Salvador, P., Alonso-Pérez, S., Pey, J., Artíñano, B., de Bustos, J., Alastuey, A., Querol, X., 2014. African dust outbreaks over the western Mediterranean Basin: 11-Year characterization of atmospheric circulation patterns and dust source areas. Atmos. Chem. Phys. 14, 6759–6775. https://doi.org/10.5194/acp-14-6759-2014.

Sanderson, P., Delgado- Saborit, J., Harrison, R.M., 2014. A review of chemical and physical characterisation of atmospheric metallic nanoparticles. Atmos. Environ. https://doi.org/10.1016/j.atmosenv.2014.05.023.

Singh, R., Sharma, B.S., 2012. Composition, seasonal variation, and sources of PM10 from world heritage site Taj Mahal, Agra. Environ. Monit. Assess. 184, 5945–5956. https://doi.org/10.1007/s10661-011-2392-0.

Stafoggia, M., Zauli-Sajani, S., Pey, J., Samoli, E., Alessandrini, E., Basagaña, X., Cernigliaro, A., Chiusolo, M., Demaria, M., Díaz, J., Faustini, A., Katsouyanni, K., Kelessis, A.G., Linares, C., Marchesi, S., Medina, S., Pandolfi, P., Pérez, N., Querol, X., Randi, G., Ranzi, A., Tobias, A., Forastiere, F., and the MED-PARTICLES Study Group, (2016). Desert dust outbreaks in Southern Europe: contribution to Daily PM10 concentrations and short-term associations with mortality and hospital admissions. Environ. Health Perspect. 124(4), 413–419. doi:https://doi.org/10.1289/ehp.1409164.

Sternbeck, J., Sjodin, A., Andreasson, K., 2002. Metal emissions from road traffic and the influence of resuspension—results from two tunnel studies. Atmos. Environ. 36, 4735–4744. https://doi.org/10.1016/S1352-2310(02)00561-7.

Styszko, K., Samek, L., Szramowiat, K., Korzeniewska, A., Kubisty, K., Rakoczy-Lelek, R., Kistler, M., Kasper Giebl, A., 2017. Oxidative potential of PM10 and PM2.5 collected at high air pollution site related to chemical composition: Krakow case study. Air Qual. Atmos. Health. https://doi.org/10.1007/s11869-017-0499-3.

Swaine, D.J., 2000. Why trace elements are important. Fuel Process. Technol. 65–66, 21–33. https://doi.org/10.1016/S0378-3820(99)00073-9.

Terrouche, A., Ali-Khodja, H., Talbi, M., Bencharif-Madani, F., Charron, A., Derradji, A., 2014. Roadside PM10 and associated metals in Constantine, Algeria. Int. J. Environ. Stud. https://doi.org/10.1080/00207233.2014.975559.

Terrouche, A., Ali-Khodja, H., Kemmouche, A., Bouziane, M., Derradji, A., Charron, A., 2015. Identification of sources of atmospheric particulate matter and trace metals in Constantine, Algeria. Air Qual. Atmos. Health 9, 69–108. https://doi.org/10.1007/s11869-014-0308-1.

Thorpe, A., Harrison, R.M., 2008. Sources and properties of non-exhaust particulate matter from road traffic: a review. Sci. Total Environ. 400, 270–282. https://doi.org/10.1016/j.scitotenv.2008.06.007.

Thurston, Splenger, G.S., 1985. A multivariate assessment of meteorological influences on inhalable particle source impacts. J. Clim. Appl. Meteorol. 24, 1245–1256.

Tian, H.-Z., Wang, Y., Xue, Z.-G., Cheng, K., Qu, Y.-P., Chai, F.-H., Hao, J.-M., 2010. Trend and characteristics of atmospheric emissions of Hg, As, and Se from coal combustion in China, 1980–2007. Atmopheric Chemistry and Physics 10, 11910–11919. https://doi.org/10.5194/acp-10-11905-2010.

Viana, M., Pandolfi, M., Minguillon, M., Querol, X., Alastuey, A., Monfort, E., Celades, I., 2008. Inter-comparison of receptor models for PM source apportionment: case study in an industrial area. Atmos. Environ. 42, 3820–3832. https://doi.org/10.1016/j.atmosenv.2007.12.056.

Viana, M., Pey, J., Querol, X., Alastuey, A., de Leeuw, F., Lükewille, A., 2014. Natural sources of atmospheric aerosols influencing air quality across Europe. Sci. Total Environ. 472, 825–833. https://doi.org/10.1016/j.scitotenv.2013.11.140.

Viana, M.M., Querol, X., Alastuey, A., 2006. Chemical characterisation of PM episodes in NE Spain. Chemosphere 62, 947–956. https://doi.org/10.1016/j.chemosphere.2005.05.048.

Von Schneidemesser, E., Stone, E.A., Quraishi, T.A., Shafer, M.M., Schauer, J.J., 2010. Toxic metals in the atmosphere in Lahore, Pakistan. Sci. Total Environ. 408, 1640–1648. https://doi.org/10.1016/j.scitotenv.2009.12.022.

Von Uexkull, O., Skerfving, S., Doyle, R., Braungart, M., 2005. Antimony in brake pads-a carcinogenic component? J. Clean. Prod. 13, 19–31. https://doi.org/10.1016/j.jclepro.2003.10.008.

Vousta, D., Samara, D., Kouimtzis, T., Ochsenkuhn, K., 2002. Elemental composition of airborne particulate matter in the multi-impacted urban area of Thessaloniki, Greece. Atmos. Environ. 36, 4453–4462. https://doi.org/10.1016/S1352-2310(02)00411-9.

Waheed, A., Zhang, Y., Bao, L., Cao, Q., Zhang, G., Li, Y., Li, X., 2010. Study of seasonal variation and source characteristic of PM10 of Shanghai urban atmosphere using PIXE. J. Radioanal. Nucl. Chem. 283, 427–432. https://doi.org/10.1007/s10967-009-0390.

Wahid, N.B.A., Latif, M.T., Suratman, S., 2013. Composition and source apportionment of surfactants in atmospheric aerosols of urban and semi-urban areas in Malaysia. Chemosphere 91 (11), 1508–1516. https://doi.org/10.1016/j.chemosphere.2012.12.029.

Wahlin, P., Berkowicz, R., Palmgren, F., 2006. Characterisation of traffic-generated particulate matter in Copenhagen. Atmos. Environ. 40, 2151–2159. https://doi.org/10.1016/j.atmosenv.2005.11.049.

Wang, H., Zhuang, Y., Wang, Y., Sun, Y., Yuan, H., Zhuang, G., Hao, Z., 2008. Long-term monitoring and source apportionment of PM2.5/PM10 in Beijing, China. J. Environ. Sci. 20 (11), 1323–1327.

Wang, Y., Zhuang, G., Sun, Y., An, Z., 2006. The variation of characteristics and formation mechanisms of aerosols in dust, haze, and clear days in Beijing. Atmos. Environ. 40, 6579–6591. https://doi.org/10.1016/j.atmosenv.2006.05.066.

WHO, 2016. Ambient Air Pollution: A Global Assessment of Exposure and Burden of Disease. 978 92 4 151135 3.

Yadav, S., Satsangi, P., 2013. Characterization of particulate matter and its related metal toxicity in an urban location in South West India. Environ. Monit. Assess. 185, 7365–7379. https://doi.org/10.1007/s10661-013-3106-6.

Yatkin, S., Bayram, A., 2008. Determination of major natural and anthropogenic source profiles for particulate matter and trace elements in Izmir, Turkey. Chemosphere 71, 685–696. https://doi.org/10.1016/j.chemosphere.2007.10.070.

Zheng, J., Zhan, C., Yao, R., Zhang, J., Liu, H., Liu, T., ... Cao, J., 2017. Levels, sources, markers and health risks of heavy metals in PM2.5 over a typical mining and metallurgical city of Central China. Aerosol Science and Engineering 2 (1), 1–10. https://doi.org/10.1007/s41810-017-0018-9.